Geoscience Frontiers 17 (2026) 102245

Contents lists available at ScienceDirect

Geoscience Frontiers

journal homepage: www.elsevier.com/locate/gsf

Research Paper

Linking Gondwana inheritance to Alpine paleogeography in the Northern Dora-Maira Massif (Western Alps)

Gianni Balestro [a], Matthieu Roà [a], Carlo Bertok [a], Marco Gattiglio [a], Stefano Ghignone [a], Chiara Groppo [a], Valby van Schijndel [b], Andrea Festa [a,*]

[a] Department of Earth Sciences, University of Torino, Via Valperga Caluso 35, 10125 Torino, Italy
[b] GFZ Helmholtz Centre for Geosciences, Telegrafenberg D-14473 Potsdam, Germany

ARTICLE INFO

Article history:
Received 22 October 2025
Revised 4 December 2025
Accepted 29 December 2025
Available online 3 January 2026

Keywords:
Pre-orogenic tectonostratigraphy
Structural inheritance
Ocean-continent transition zone
Western Alps
Dora-Maira Massif

ABSTRACT

Inherited structures in rifted continental margins strongly influence the architecture and evolution of collisional orogens. The northern Dora-Maira Massif in the Western Alps (NW Italy) preserves records of such inheritances, capturing the transition from Gondwana inheritance to Alpine convergence. New lithostratigraphic and structural data, together with U–Pb zircon dating, reveal a long-lasting tectonostratigraphic and/or magmatic evolution during (i) pre-Permian, (ii) Permian, (iii) Triassic and (iv) Jurassic time intervals. The heterogeneous Paleozoic basement consists of pre-Variscan micaschist and metabasite, and was intruded by Permian igneous bodies now corresponding to the Borgone metagranite and Luserna augen gneiss. The basement was later overlain by a Mesozoic cover made up of Lower Triassic siliciclastic sediments, a Middle to Upper Triassic carbonate platform and Lower to Middle Jurassic *syn*-rift deposits linked to the opening of the Ligurian–Piedmont Ocean Basin. Our results highlight that the Dora-Maira Massif was located within a transitional paleogeographic domain, emphasizing the role of pre-rift architecture in governing margin segmentation. Successive cycles of sedimentation, magmatism, and rifting created structural and rheological heterogeneities that may have localized strain during the Cenozoic Alpine-related overprinting. The Dora-Maira case illustrates that deep-time inherited structures and tectonostratigraphic settings continue to influence rifting, subduction, and collision, offering a broader framework for understanding the dynamics of orogens worldwide.

© 2025 China University of Geosciences (Beijing) and Peking University. Published by Elsevier B.V. on behalf of China University of Geosciences (Beijing). This is an open access article under the CC BY-NC-ND license (http://creativecommons.org/licenses/by-nc-nd/4.0/).

1. Introduction

Research on plate convergence zones increasingly highlights the role of inherited (i.e., pre-orogenic) structures and tectonostratigraphic settings in shaping the evolution of orogens, from pre-orogenic stages through subduction and collision (e.g., Erdos et al., 2014; Pfiffner, 2017; Yang, 2022). The Alps provide a key example showing how the reconstructions of their tectonic history depend on the architecture of the European and Adria paleomargins and the intervening Ligurian-Piedmont Ocean Basin (Butler et al., 2006; Mohn et al., 2014; Festa et al., 2020). Following oceanic lithosphere consumption, the tectonic incorporation of the European rifted margin was pivotal in the transition from subduction to collision, through basal décollement propagation (Tavani et al., 2021) and subsequent tectonic underplating (Platt, 1986). Reconstructions of the European and Adria paleomargins, especially when integrating pre-rift architectures and basement-cover interfaces, have been essential in decipher the complex structure of the Western Alps (Ballèvre et al., 2018; Manatschal et al., 2022). Understanding how pre-existing structures influenced rift propagation and margin segmentation is therefore critical to constrain the mechanical behaviour of the lithosphere during orogeny. Inherited crustal heterogeneities, such as fault zones, heterogeneous stratigraphic successions with internal lithological contrasts and rheological anisotropies, commonly localize strain and guide the architecture and evolution of accretionary complexes, metamorphic gradients, and exhumation pathways during subsequent collisional stages. Consequently, deciphering the nature and distribution of these inherited features is key to building robust geodynamic models of orogenic belts.

In this work, we present new lithostratigraphic and chronostratigraphic constraints on the Paleozoic to Mesozoic evolution of the northernmost sector of the Dora-Maira Massif in the Western Alps (NW Italy; Fig. 1a, b). This Massif, famous for the first discovery of coesite-bearing ultra-high pressure mineral assemblages

* Corresponding author.
E-mail address: andrea.festa@unito.it (A. Festa).

https://doi.org/10.1016/j.gsf.2025.102245
1674-9871/© 2025 China University of Geosciences (Beijing) and Peking University. Published by Elsevier B.V. on behalf of China University of Geosciences (Beijing). This is an open access article under the CC BY-NC-ND license (http://creativecommons.org/licenses/by-nc-nd/4.0/).

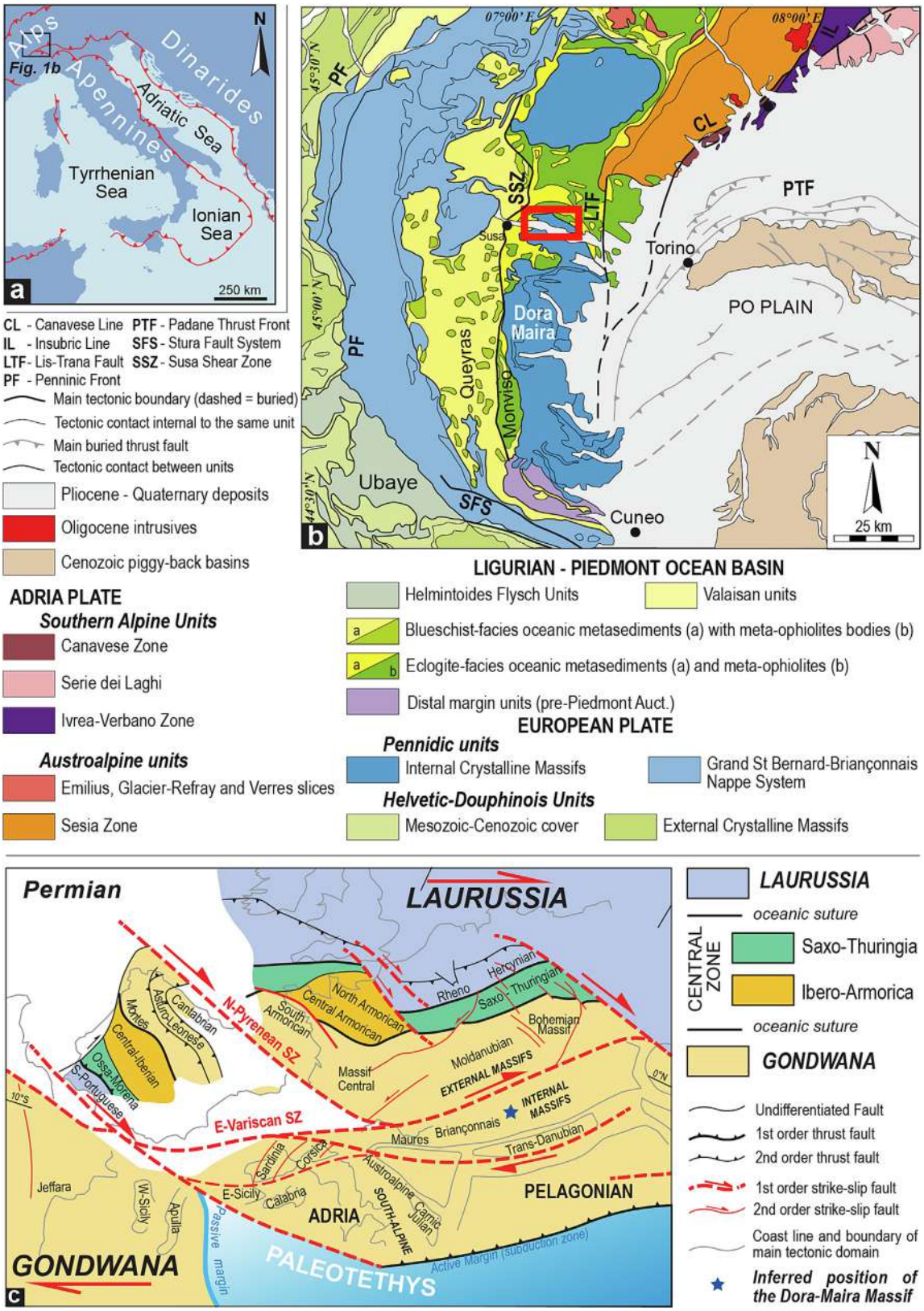

Fig. 1. (a) Sketch of the Alps-Apennine orogenic system and location of the map shown in Fig. 1b. (b) Tectonic scheme of the Western Alps (modified after Balestro et al., 2015): the red square indicates the study area. (c) Paleogeographic reconstruction of the Variscan Belt at Early Permian, showing the inferred position of the Dora Maira Massif (modified from: Stampfli et al., 2002; Schettino and Turco, 2011; Ballèvre et al., 2018; Festa et al., 2020).

(Chopin, 1984), remains central to debates on Alpine geodynamics. Our results demonstrate that, despite Alpine deformation and metamorphism overprinting, both the Paleozoic basement and the Mesozoic cover succession preserve relicts of their pre-orogenic tectonostratigraphic evolution, linking the transition from Gondwana inheritance to Alpine paleogeography (Fig. 1c). Reconstructing this evolution allows us to define a heterogeneous pre-orogenic architecture of the distal and hyperextended European rifted margin, an architecture that must be considered when interpreting the tectono-metamorphic evolution of the Western Alps. Geological mapping and multiscale lithostratigraphic analysis in low strain domains reveal a complex pre-Alpine tectonic framework, which we compare with others Western Alpine units, yielding new insights into rift-related paleogeography. These findings not only help to better constrain the inherited Paleozoic – Mesozoic tectono-stratigraphic architecture, but also emphasize its influence on the Alpine deformation pattern, contributing to a broader understanding of how deep-time processes shape collisional orogens.

2. Geological setting

The Western Alps resulted from the Cenozoic collision between the Adria upper plate and the European lower plate, following consumption of the oceanic lithosphere of the Jurassic-Cretaceous Ligurian-Piedmont Ocean Basin (Coward and Dietrich, 1989; Rosenbaum and Lister, 2005; Handy et al., 2010). The orogenic belt mainly formed through (i) Late Cretaceous accretion of the thinned Adriatic margin, (ii) oblique subduction of oceanic lithosphere during the Paleocene to Eocene, and (iii) multiple collisions in the Eocene – Oligocene involving the Briançonnais microcontinent and, later, the European continent (Platt et al., 1989; Butler et al., 2013). The axial zone of the Western Alps (Fig. 1b) developed as a double-verging accretionary wedge, driven by deep crust-mantle indentation (Malusà et al., 2011; Schmid et al., 2017), and incorporating terranes from the Adriatic margin (i.e., the Austroalpine units), the European/Briançonnais margins, and the intervening Ligurian-Piedmont Ocean Basin (Beltrando et al., 2010; Marroni et al., 2010; Balestro et al., 2019).

The Europa-derived units have been interpreted as part of the northern Gondwana palaeomargin (von Raumer et al., 2013; Siegesmund et al., 2021; Linnemann, 2025) (Fig. 1c). Those exposed in the axial sector of the belt (i.e., the Grand St Bernard-Briançonnais Nappe System and the Internal Crystalline Massifs; e.g., Ballèvre et al., 2018), recorded complex deformation and metamorphic histories through different orogenic cycles (i.e., the Alpine, Variscan and pre-Variscan cycles; Rosenberg and Bellahsen, 2024, and references therein). The Grand St Bernard-Briançonnais Nappe System consists of (i) polycyclic Variscan and pre-Variscan rocks (Bergomi et al., 2017; Maino et al., 2018), (ii) Permian igneous bodies, (iii) Upper Carboniferous to Lower Triassic siliciclastic metasediments and (iv) Middle Triassic to Eocene carbonate ones (i.e., the classic cover succession of the Briançonnais Zone; Lemoine et al., 1986; Decarlis et al., 2013). These lithostratigraphic features similarly characterize the Internal Crystalline Massifs (i.e., Dora-Maira, Gran Paradiso and Monte Rosa massifs; Dal Piaz et al., 2003; Gasco et al., 2013) but, in these ones, the Mesozoic cover successions are almost poorly preserved.

The Dora-Maira Massif (DMM; Fig. 1b) is characterized by a very complex tectonic setting and, although generally considered a distal part of the Briançonnais microcontinent (Schmid et al., 2004), its precise paleogeographic position has been debated and a provenance from the Adria upper plate was also hypothesized (Polino et al., 1990). Subduction timing is diachronous across DMM with Alpine metamorphic P-T peak conditions ranging from Paleocene – Early Eocene in the northern part (Manzotti et al., 2025a) to the Eocene – Oligocene transition in more intensively studied southern areas (e.g., Tilton et al., 1989; Rubatto and Hermann, 2001; Chen et al., 2016). Furthermore, after the first discovery of coesite-bearing ultra-high pressure mineral assemblages (Chopin, 1984), other occurrences of coesite-bearing rocks were found (Manzotti et al., 2022; Groppo et al., 2025; Manzotti et al., 2025b), raising new questions about the internal structural architecture of the whole DMM.

At present, the DMM presents an elongated and dome-like shape that juxtaposes several tectonic units (i.e., the different 'Ensembles' of Vialon (1966)) with distinct pre-Alpine stratigraphy and differing Alpine P-T peak conditions (Henry et al., 1993; Sandrone et al., 1993; Hermann, 2003; Di Vincenzo et al., 2006; Castelli et al., 2007; Groppo et al., 2019). The lowermost unit, the Pinerolo Unit, records blueschist-facies P-T peak conditions (Borghi et al., 1984; Avigad et al., 2003), and mainly consists of Upper Carboniferous metasediments intruded by Lower Permian dioritic to granitic plutons (Bussy and Cadoppi, 1996; Manzotti et al., 2016). Overlying are several quartz-eclogite and coesite-eclogite facies tectonic units (Chopin et al., 1991; Compagnoni et al., 2012; Bonnet et al., 2022; Groppo et al., 2025; Manzotti et al., 2025b). Their Variscan basement consists largely of pre-Carboniferous pelitic-arenaceous metasediments, minor marble and mafic rocks (Groppo et al., 2007; Cadoppi et al., 2016; Ferrando et al., 2017), intruded by Ordovician orthogneiss (Bussy and Cadoppi, 1996; Nosenzo et al., 2024). This composite basement also hosts widespread Permian granitoids (Bussy and Cadoppi, 1996; Gebauer et al., 1997; Gauthiez-Putallaz et al., 2016; Chen et al., 2023; Nosenzo et al., 2024). In the southernmost sector, eclogite-facies units are tectonically overlain by the blueschist-facies Dronero Unit (Michard et al., 1993; Balestro et al., 2020), which includes polycyclic metasediments, *meta*-intrusive bodies, and monocyclic metasediments locally interlayered with Permian metavolcanics (Michard and Vialon, 1966; Bonioli et al., 1992; Balestro et al., 2022a). The Mesozoic cover succession is almost preserved in the northernmost DMM (i.e., area of present study), whereas along the western flank of the dome is tectonically sliced (Balestro et al., 2013). In sectors adjoining the southern DMM, the cover successions occur in a detached, upright nappe stack (i.e., pre-Piedmont successions of the ocean-continent transition zone; Balestro et al., 2022a).

The sector we investigated in the northern DMM, along the Susa Valley (Fig. 1b), is tectonically separated from the overlying Susa and Lanzo valleys *meta*-ophiolites (Festa et al., 2021; De Togni et al., 2024) by the Foresto Shear Zone (Fig. 2). It consists of a Paleozoic basement and a Mesozoic cover now juxtaposed along the Bussoleno Detachment Zone (Balestro et al., 2025a). Metamorphic P-T peak in the northernmost DMM reached eclogite-facies conditions (Gasco et al., 2011). Deformation during the Alpine cycle comprises four main deformation phases, corresponding to the subduction-related D1 phase and the early (D2) to late (D3 and D4) exhumation-related phases (Tallone, 1988; Cadoppi et al., 2002; Gasco et al., 2011; Balestro et al., 2025a). Syn-metamorphic folding and shearing stages were followed by a post-metamorphic faulting stage (Perrone et al., 2010).

3. Methods

The study area has been investigated by (i) field-based methods, namely geological mapping and mesoscale lithostratigraphic analyses, (ii) microscale petrographic characterization of selected samples, (iii) whole-rock geochemistry and (iv) U–Pb geochronology.

Bulk-rock compositions were determined via ICP-MS analyses by ALS Company (details about standard and methods at https://

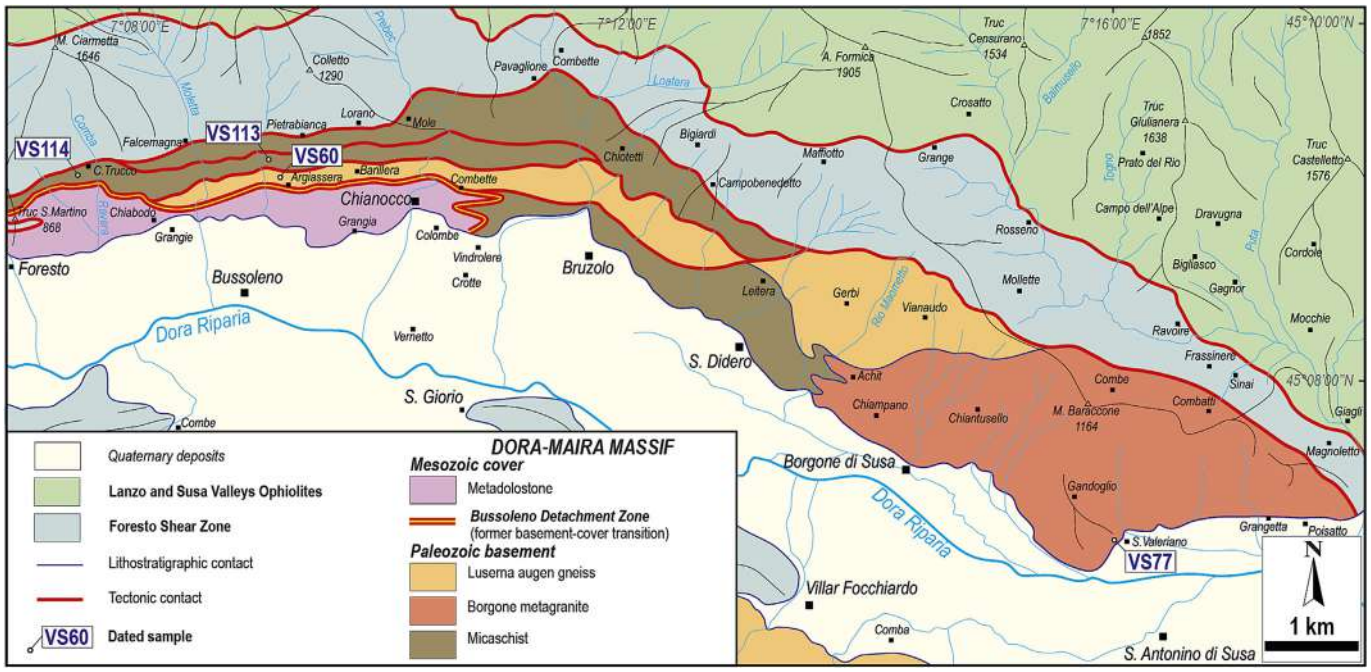

Fig. 2. Geological map of the study area (modified after Cadoppi et al., 2002; and Balestro et al., 2025a) with the location of the dated samples.

www.alsglobal.com/en/geochemistry) and SEM-EDS areal analyses. The latter is performed using a JEOL IT300LV scanning electron microscope (Department of Earth Sciences, University of Torino, Italy), equipped with an Energy 200 energy-dispersive spectrometry (EDS) and an X- Act3 silicon drift detector (Oxford Inca Energy). Analytical conditions included a 15 kV acceleration voltage, 10 mm working distance, 35 s counting time, with 25–30 analyses per sample at 50× magnification. Geochemical analyses were used to determinate: (i) the major-element composition and Chemical Index of Alteration (CIA; Nesbitt and Young, 1982) of magmatic rocks (Table 1), and (ii) the approximate mineralogical compositions of sedimentary protoliths (Table 2), following the method of Groppo et al. (2021) and Tamang et al. (2024). For the latter, the following assumptions were adopted: (i) CaO from the silicate fraction (CaO*) is equivalent to Na_2O and is incorporated in anorthite (the remaining CaO_{carb} is incorporated into carbonates, calcite and/or dolomite); (ii) FeO enters only in chlorite or, alternatively in siderite; (iii) albite incorporates all the Na_2O. The modal proportions of the protolith minerals were obtained using the least-squares method (PCalc; Godard, 2009) and using end-member compositions and molar volumes for kaolinite, illite, clinochlore, daphnite, albite, anorthite, quartz, K-feldspar, calcite, dolomite and siderite (Table 2).

Chronostratigraphic constraints are provided by U–Pb geochronology (see Section 5), with ages of protoliths referenced to the International Chronostratigraphic Chart by Cohen et al. (2013, updated). Details about sample preparation and LA-ICP-MS analytical conditions, together with data files, are available at the Data Service of Helmholtz Centre for Geosciences (Balestro et al., 2025b).

4. Lithostratigraphy

A Paleozoic basement and an overlying Mesozoic metasedimentary cover characterize the inferred pre-Alpine stratigraphic succession of the northernmost sector of the DMM (Fig. 3). The basement consists of pre-Variscan micaschist and metabasite (Cadoppi and Tallone, 1992; Gasco et al., 2011), and different

Table 1
Major element composition of magmatic rocks from the northernmost Dora-Maira Massif and related Chemical Index of Alteration (CIA).

	Borgone metagranite			Luserna massive gneiss			Luserna banded gneiss		
Sample	**VS50**[a]	**VS77**[a]	**VSU67**[b]	**VS54**[a]	**VS60**[a]	**VSU53**[b]	**VS103**[a]	**VS58**[a]	**PV1273**[c]
Lat.	45°09′06″ N	45°06′54″ N	45°07′37″ N	45°08′55″ N	45°08′06″ N	45°08′29″ N	45°08′02″ N	45°07′25″ N	45°07′29″ N
Long.	7°08′28″ E	7°15′52″ E	7°13′59″ E	7°08′11″ E	7°09′09″ E	7°08′11″ E	7°13′22″ E	7°08′24″ E	7°08′38″ E
SiO_2	72.60	73.60	74.49	72.10	71.40	71.74	74.30	71.80	75.35
TiO_2	0.24	0.12	0.22	0.30	0.31	0.22	0.20	0.10	0.05
Al_2O_3	13.10	13.05	13.30	14.40	14.25	13.91	13.45	11.8	13.60
$Fe_2O_3^t$	2.84	2.01	2.04	3.31	3.04	2.12	2.71	2.41	1.75
MnO	0.05	0.05	0.04	0.06	0.05	0.05	0.05	0.03	0.05
MgO	0.49	0.30	0.30	0.59	0.55	0.40	0.77	2.94	0.65
CaO	0.53	0.38	0.96	1.00	1.18	1.31	0.39	1.03	0.55
Na_2O	2.57	3.34	2.91	3.25	3.32	3.34	3.20	0.11	2.95
K_2O	5.22	4.78	5.09	5.28	4.98	5.16	3.62	5.99	3.50
P_2O_5	0.12	0.12	0.17	0.14	0.14	0.17	0.13	0.02	0.20
LOI	1.08	0.66	0.75	0.83	0.95	1.35	1.16	2.53	0.65
Total	98.84	98.41	100.27	101.26	100.17	99.77	99.98	98.76	99.30
CIA	**55.4**	**54.1**	**53.3**	**53.4**	**52.9**	**51.6**	**58.4**	**58.2**	**59.7**

Note: a – this work; b – Cadoppi, 1990; c – Vialon, 1966.

Table 2
Bulk compositions (mol.%) of pre-rift metasediments from the northernmost Dora-Maira Massif and related approximate mineral composition (vol.%) of protoliths.

	Quarzite		Quartzschist	Carbonate micaschist		Marble	Dolomitic marble	Metadolostone
Sample	**RS24**[a,1]	**2520**[a,1]	**RS6**[a,1]	**245**[a,1]	**VS132**[a,1]	**RS3**[a,1]	**244**[a,1]	**40–4**[b,2]
Lat.	5°08′57″ N	45°16′52″ N	45°09′12″ N	45°08′40″ N	45°08′45″ N	45°08′48″ N	45°08′37″ N	45°08′35″ N
Long.	7°07′55″ E	7°16′59″ E	7°08′30″ E	7°07′26′'	7°07′21″ E	7°08′05″ E	7°07′02″ E	7°06′57″ E
SiO_2	94.30	93.61	77.99	80.94	78.11	5.89	3.22	1.00
TiO_2	0.07	0.05	0.38	0.36	0.36	0.02	0.33	0.01
Al_2O_3	3.21	3.44	8.65	9.33	10.59	0.81	0.94	0.29
FeO_{tot}	0.36	0.48	4.83	2.73	3.35	0.35	1.10	0.04
MnO	0.01	0.00	0.08	0.14	0.16	0.01	0.00	0.00
MgO	0.52	0.67	3.22	1.75	2.05	17.55	41.89	46.99
CaO	0.10	0.76	1.20	0.81	0.75	75.06	52.23	51.60
Na_2O	0.18	0.10	1.39	0.40	1.13	0.05	0.03	0.00
K_2O	1.25	0.88	2.25	3.54	3.50	0.26	0.26	0.07
Total	100	100	100	100	100	100	100	100
CaO*	0.10	0.10	1.20	0.40	0.75	0.05	0.03	0.00
CaO_{carb}	0.0	0.66	0.00	0.41	0.00	75.01	52.20	51.60
Protoliths (vol.%)								
Ill	10	14	14	25	25	3.0	3.0	0.0
FeChl	1.0	1.0	9.0	5.0	6.0	0.0	1.0	0.0
MgChl	1.0	1.0	6.0	3.0	4.0	0.0	0.0	1.0
Qz	81	82	44	46	38	3.0	1.0	0.0
Cal	0.0	1.0	0.0	1.0	0.0	60	11	6.0
Dol	0.0	0.0	0.0	0.0	0.0	35	85	93
Ab	2.0	1.0	12	3.0	9.0	0.0	0.0	0.0
Kfs	6.0	0.0	12	16	15	0.0	0.0	0.0
An	0.0	0.0	5.0	2.0	3.0	0.0	0.0	0.0

Note: CaO* = CaO from the silicate fraction. CaO_{carb} = CaO from the carbonate fraction; a – this work; b – Compagnoni et al., 2003; 1 – SEM-EDS analysis; 2 – ICP-MS analysis. Protoliths abbreviations: Ill – Illite, FeChl – Iron chlorite, MgChl – Magnesium chorite, Qz – Quartz, Cal – Calcite, Dol – Dolomite, Ab – Albite, Kfs – K-feldspar, An – Anorthite.

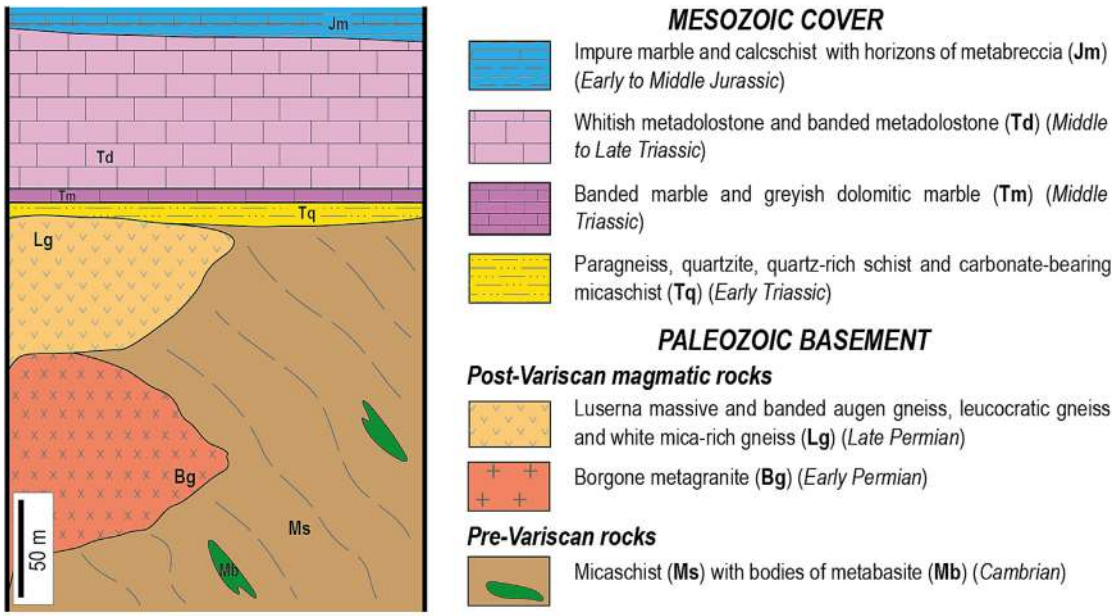

Fig. 3. Pre-Alpine columnar section showing the stratigraphic relationships between the different lithological units of the northernmost Dora Maira Massif.

augen gneisses (i.e., the Luserna-type gneiss and the Borgone metagranite of Cadoppi et al. (2002)). The cover succession is preserved both in direct contact with the basement (Cadoppi and Tallone, 1992; Fudral, 1996), partly detached along the Bussoleno Detachment Zone, and as tectonically sampled megablocks, which are embedded within the Cretaceous calcschist of the Foresto Shear Zone (Balestro et al., 2025a). The margins of these megablocks locally include thin marble horizons of Jurassic age (Fudral et al., 1994). The Mesozoic succession is subdivided into (i) a Lower Triassic heterogeneous succession of paragneiss, quartzite, quartz-rich schist and carbonate-bearing micaschist, marking the basement-cover transition, (ii) Middle to Upper Triassic marble and metadolostone, and (iii) Lower to Middle Jurassic impure marble and calcschist. The Lower Triassic heterogeneous succession acted as a major Alpine detachment zone (Balestro et al., 2025a), and its lithostratigraphy has been reconstructed mainly from almost preserved primary contacts within composite tectonic slices.

4.1. Pre-Variscan rocks

Pre-Variscan rocks consist of few hundred of metres-thick micaschist with minor bodies of metabasite (Fig. 3). The micaschist is typically brownish-grey in colour and coarse-grained (Fig. 4a, b),

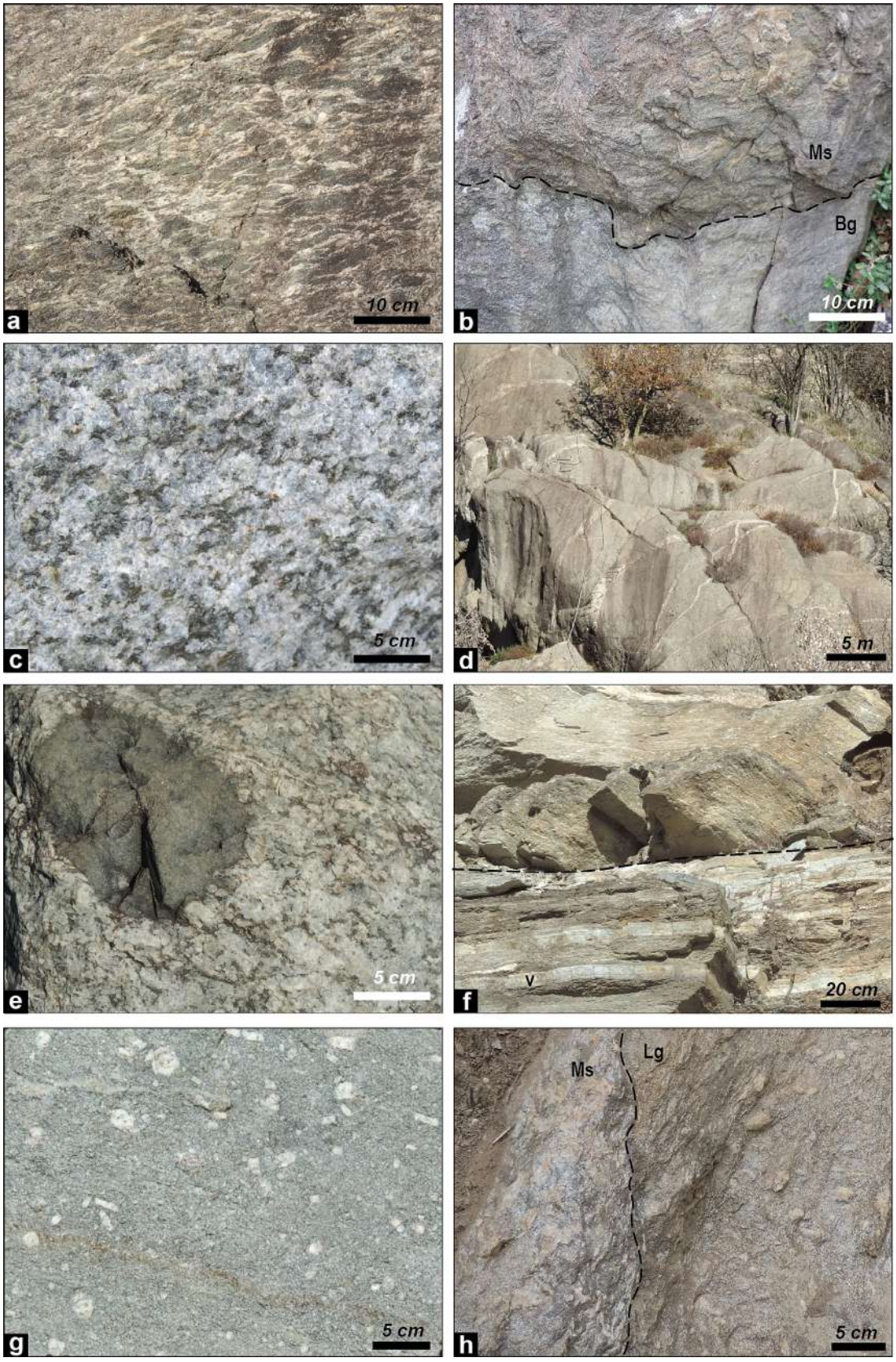

Fig. 4. Field images of the Paleozoic lithostratigraphic units. (**a**) Close-up view of the pre-Variscan micaschist and related coarse-grained fabric (C. Trucco). (**b**) Outcrop view of a primary contact (dashed black line) between the pre-Variscan micaschist (Ms) and Borgone metagranite (Bg) (Chiampano). (**c**) Close up view of the Borgone metagranite showing a well-preserved magmatic texture (Borgone). (**d**) Panoramic view of the Borgone metagranite crosscut by poorly oriented aplite and pegmatite dykes (Poisatto). (**e**) Close up view of an undeformed mafic enclave included in the Borgone metagranite (Poisatto). (**f**) Outcrop view of a contact (dashed black line) between the Luserna massive gneiss (above) and the banded one (below) with quartz veins (v) (Argiassera). (**g**) Close up view of the Luserna massive augen gneiss showing a well-preserved porphyroclastic texture (Argiassera). (**h**) Close up view of a contact (dashed black line) between the pre-Variscan micaschist (Ms) and Luserna augen gneiss (Lg) (Achit).

reflecting deformation and recrystallization of pre-Variscan sedimentary protoliths. The Alpine mineral assemblage mainly consists of quartz, phengite (i.e., K-rich white mica with Si > 3.20 a.p.f.u. on the basis of 11 oxygens), garnet and chloritoid. Garnet and chloritoid commonly form centimetre-sized lenticular aggregates, wrapped by millimetre-thick quartz- and white mica-rich layers. Centimetre- to decimetres-thick quartz veins are widespread throughout the micaschist.

Metabasite occurs as metre-scale, elongated bodies, typically greenish and fine-grained, with a well-developed banded fabric. The dominant mineral phases are albite, epidote, chlorite and amphibole. In some cases, relicts of a high-pressure Alpine mineral assemblage are preserved, comprising garnet, omphacite, rutile, Na-amphibole, zoisite and phengite (i.e., the Rio Maometto eclogite; Pognante and Sandrone, 1989). The scattered occurrence and sharp contacts with the surrounding micaschist suggest these metabasite represent pre-Variscan mafic dykes.

To test the pre-Variscan attribution of the micaschists, we performed a geochronological study on two samples of micaschists (see section 5.1).

4.2. Borgone metagranite

The Borgone metagranite forms a kilometre-scale, elongated body exposed in the eastern part of the study area (Fig. 2). It primarily consists of a coarse-grained, weakly foliated metagranite (Fig. 4c), locally transitioning into foliated augen gneiss. Its widely preserved equigranular magmatic texture consists of (i) centimetre-sized euhedral porphyroclasts of K-feldspar, (ii) relicts of primary biotite, and (iii) textural relicts of quartz and plagioclase. Magmatic muscovite has also been described (Cadoppi, 1990). The Alpine metamorphic overprint is mainly represented by phengite, albite and clinozoisite. Numerous *meta*-aplite and *meta*-pegmatite dykes, also locally found in the surrounding micaschist, cut the metagranite (Fig. 4d). These dykes are decimetre-thick and often poorly oriented by Alpine-related deformation. Rounded mafic enclaves of tonalitic composition (Cadoppi, 1988), up to decimetres in size (Fig. 4e), and decimetre-thick quartz veins are also present. CIA values for the metagranite range from 53 to 55 (Table 1), typical of unaltered or weakly altered acid magmatic rocks (Nesbitt and Young, 1982).

The Borgone metagranite intrudes the above-described micaschist (Fig. 3), and therefore is a good target for constraining the tectonostratigraphic evolution by U-Pb zircon dating (see Section 5.2).

4.3. Luserna gneiss

The Luserna augen gneiss varies from few tens to several hundreds of metres in thickness and consists of two main lithotypes (Fig. 4f, g, h): a massive, homogeneous gneiss, and a banded, heterogeneous one. The massive gneiss is coarse-grained and mostly weakly foliated (Fig. 4g), preserving a magmatic texture with centimetre-sized K-feldspar porphyroclasts within a medium- to fine-grained grey matrix composed primarily of quartz, phengite, albite and clinozoisite. This unit locally grades into a finer-grained, pervasively foliated augen gneiss. The banded gneiss is interlayered with the massive type and displays a prominent flaggy structure. It consists of medium-grained grey augen gneiss, quartz-rich leucocratic gneiss and greenish grey white mica-rich gneiss. Its mineral assemblage is similar to the massive one but with a higher content of white mica. K-feldspar porphyroclasts range from centimetre-sized euhedral to millimetre-sized subhedral grains. Sub-rounded aggregates of quartz, K-feldspar, albite and white mica, likely representing recrystallised tabular K-feldspar megacrysts, also occur. The banded gneiss also contains light-blue centimetre- to decimetre-thick quartz veins (Fig. 4f).

CIA values differ between the two gneiss types, with lower values for the massive gneiss (51–53) compared to the banded gneiss (58–59) (Table 1), indicating unaltered and moderately altered conditions, respectively (Nesbitt and Young, 1982). Luserna gneiss differs from the Borgone metagranite in its greater compositional heterogeneity. Lithostratigraphic and compositional features indicate that the massive gneiss originated from a felsic magmatic protolith (see Section 5.3). The origin of the banded gneiss is more complex and is addressed in detail in Section 6.2, in the context of the emplacement history of the Luserna gneiss in the upper part of the Paleozoic basement.

4.4. Lower Triassic cover succession

The transition from the Paleozoic basement to the Mesozoic metasedimentary cover is marked by a heterogeneous succession of paragneiss, quartzite, quartz-rich schist and carbonate-bearing micaschist (Fig. 3).

The paragneiss is locally interlayered with quartzite and features millimetres-sized clasts of quartz and of K-feldspar, locally showing graded sedimentary textures (Fig. 5a). The quartzite is fine- to medium-grained, and typically whitish in colour (Fig. 5b), and composed predominantly of quartz with minor white mica of both phengite and muscovite composition. Kyanite and chloritoid may also occur in the mineral assemblage (see also Tallone, 1990). Some quartzite layers are dark grey and enriched in Fe-Mn oxides. Carbonate-bearing quartzite occurs at the transition to the overlying quartz-rich schist and carbonate-bearing micaschist (Fig. 5c). These latter lithologies are locally interlayered with centimetre-thick levels of yellowish marble. The quartz-rich schist differs from the quartzite by its higher white mica content and for the occurrence of garnet. The carbonate-bearing micaschist consists of quartz, phengite, garnet, chloritoid, epidote, amphibole. Carbonate minerals occur as lozenge-shaped aggregates of calcite and Fe-oxide, interpreted as pseudomorphs after primary ankerite or siderite.

These lithologies represent a heterogeneous stratigraphic interval, varying in thickness from few metres up to approximatively twenty metres, and interpreted to derive from pebbly quartz-arenite, quartz-arenite, and quartz-rich to carbonate-bearing pelitic sediments. Bulk-rock compositions (Table 2) support that quartz-arenites are composed mainly of quartz (~80 vol%), with minor phyllosilicates (illite + chlorite = 12–16 vol%) and low amounts of K-feldspar + plagioclase contents (1–8 vol%). The pelites consist of quartz (38–46 vol%), phyllosilicates (illite + chlorite = 29–35 vol%), feldspars (plagioclase + K-feldspar = 21–29 vol%), and minor carbonate (<5 vol%).

The basal part of this heterogeneous succession, corresponding to the quartz-arenite, is assigned to the Early Triassic based on lithostratigraphic correlation with equivalent siliciclastic successions in the Alps and Apennines (e.g., Cassinis et al., 2018). Regional chronostratigraphic correlations are presented and discussed further (Section 6.3.1).

4.5. Middle to upper Triassic cover succession

Above the Early Triassic heterogeneous succession, the cover succession continues with metadolostone up to one hundred of meters thick. The basal portion includes a few metres of banded marble passing upward to dolomitic marble. The banded marble is massive and shows a banded texture defined by alternating whitish grey and dark grey levels (Fig. 5c). At the microscale, this is expressed as compositional layering of dolomite-rich and calcite-rich levels, with minor quartz and white mica. Relicts of saddle-dolomite crystals are also present (Fig. 5d). The dolomitic marble is grey in colour and consists primarily of dolomite and calcite (Fig. 5e), with minor amounts of phengite, paragonite, quartz, epidote and chlorite. It

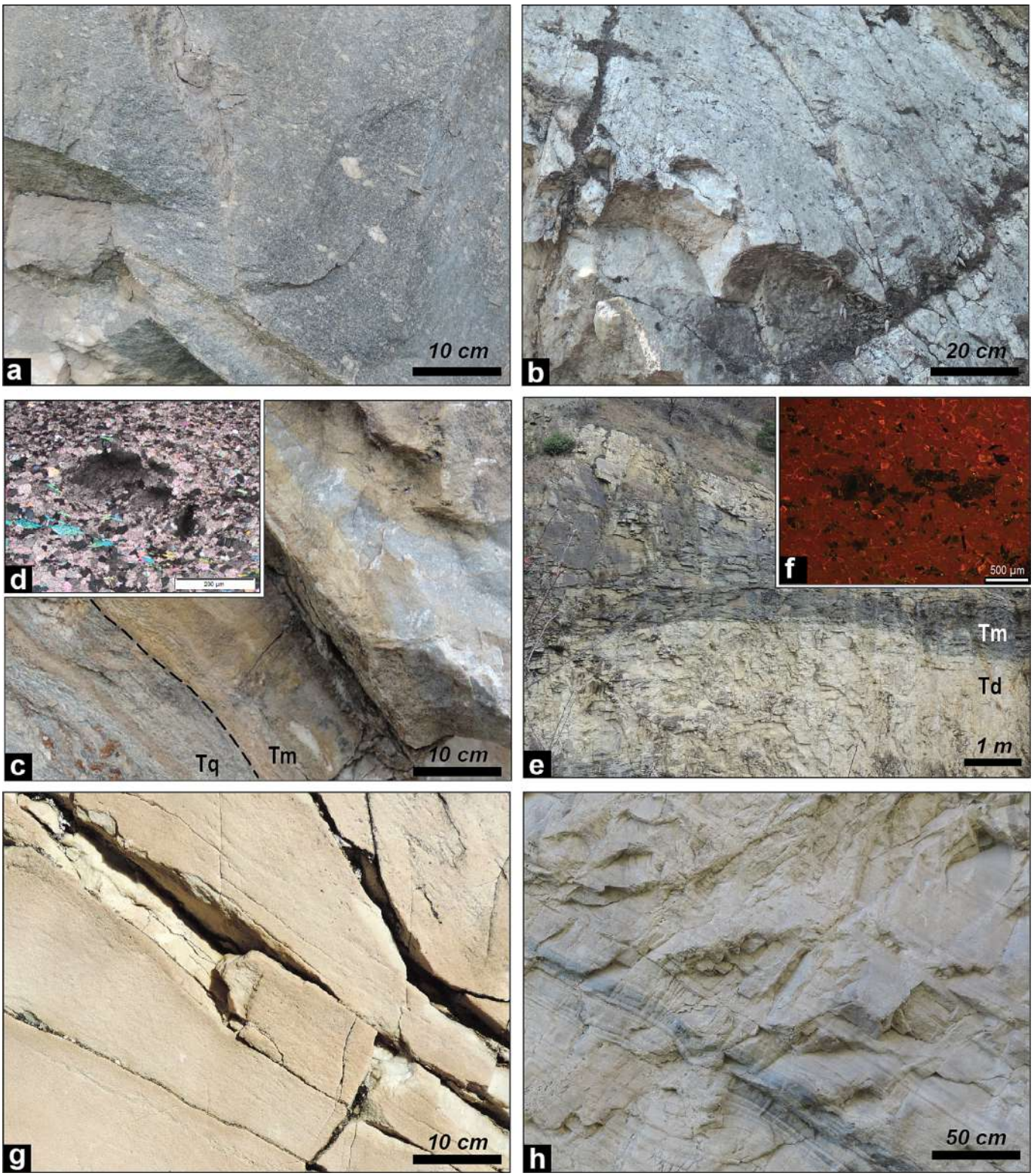

Fig. 5. Field and microscale images of the Triassic lithostratigraphic units. (**a**) Close-up view of the paragneiss with millimetres-sized clasts of quartz and K-feldspar showing graded sedimentary textures (Combe). (**b**) Whitish quartzite of the basement-cover transition (North of Grangie). (**c**) Close-up view of the contact (dashed black line) between the carbonate-bearing micaschist (Tq) and the banded marble (Tm), occurring at top of the basement-cover transition and at bottom of the carbonate cover, respectively (Chiabodo). (**d**) Microscale detail of a saddle-dolomite crystal occurring in the banded marble (cross-polarized light). (**e**) View of contacts between the grey dolomitic marble (Tm) and whitish dolostone (Td) (East of Foresto). (**f**) Microscale texture of the grey dolomitic marble consisting of granoblastic dolomite (red) and irregular aggregates of calcite (dark grey) interpreted as cement-filled primary shrinkage pores (cathodoluminescence). (**g**) Close-up view of the homogenous whitish metadolostone (East of Foresto). (**h**) View of the banded metadolostone with a fetid grey layer (Foresto).

shows a homogeneous, granoblastic texture consisting of dolomite, while calcite is mostly concentrated in irregular, sub-millimetre domains, likely representing cement-filled primary shrinkage pores (Fig. 5f). The limestone and calcareous dolostone protoliths were originally composed of calcite (60 vol%) and dolomite (35 vol%), with minor quartz and illite (~5 vol%), and of dolomite (85 vol%), calcite (11 vol%), and accessory phyllosilicates (~4 vol%) and quartz (~1 vol%), respectively (Table 2).

The metadolostone varies stratigraphically from homogenous whitish facies at the base (Fig. 5g) to a banded one at the top (Fig. 5h). The banded metadolostone is made up of centimetres-thick layers, varying in colour from light grey to pinkish grey, or fetid dark grey. The mineral assemblage is dominated by dolomite with minor phengite. Bulk-rock compositions (Table 2) reflect a protolith dominated by dolomite (93 vol%), with minor calcite (6 vol%) and trace chlorite (~1 vol%). Based on the occurrence of recrystallized crinoid fragments (undetermined; Franchi, 1898), the metadolostone is generally considered to be of Middle to Late Triassic age.

4.6. Lower to Middle Jurassic cover succession

The above-described metadolostone is locally overlain by impure marble and calcschist, which reach thickness of up to a ten of metres (Fig. 6a). The light grey impure marble and the grey-brown calcschist occur as decimetre-thick interlayered horizons and are compositionally similar, but the calcschist contains more quartz and white mica, and less calcite. Quartz-veins and, locally, centimetre-thick layers of blackish micaschist are also present.

Notably, the impure marble and calcschist are also interlayered by horizons of two types of metabreccia. The first type occurs as decimetres-thick layers and is either clast- or matrix-supported (Fig. 6b–d). This metabreccia consists of centimetres-sized bluish clasts made up of coarse-grained calcite crystals, angular to sub-rounded in shape, embedded in a light grey matrix dominated by fine-grained calcite, quartz, and white mica (Fig. 6b). Textural and compositional features suggest that these aggregates originated as primary intraclasts. The second type of metabreccia is matrix-supported and consists of metres-thick levels with up to decimetre-sized clasts of dolomitic composition (Fig. 6e), showing same characteristics of the above-described metadolostone. The impure marble and calcschist derive from marly limestone and are thus characterized by the occurrence of reworked carbonate material. Such features are diagnostic of metasedimentary successions described throughout the Western Alps and deposited between the upper part of the Early Jurassic and the Middle Jurassic (Michard, 1967; Decarlis et al., 2013).

5. U-Pb geochronology

5.1. Pre-Variscan micaschists

Zircon crystals were separated from two samples of pre-Variscan micaschist (VS113 and VS114), in order to infer the max-

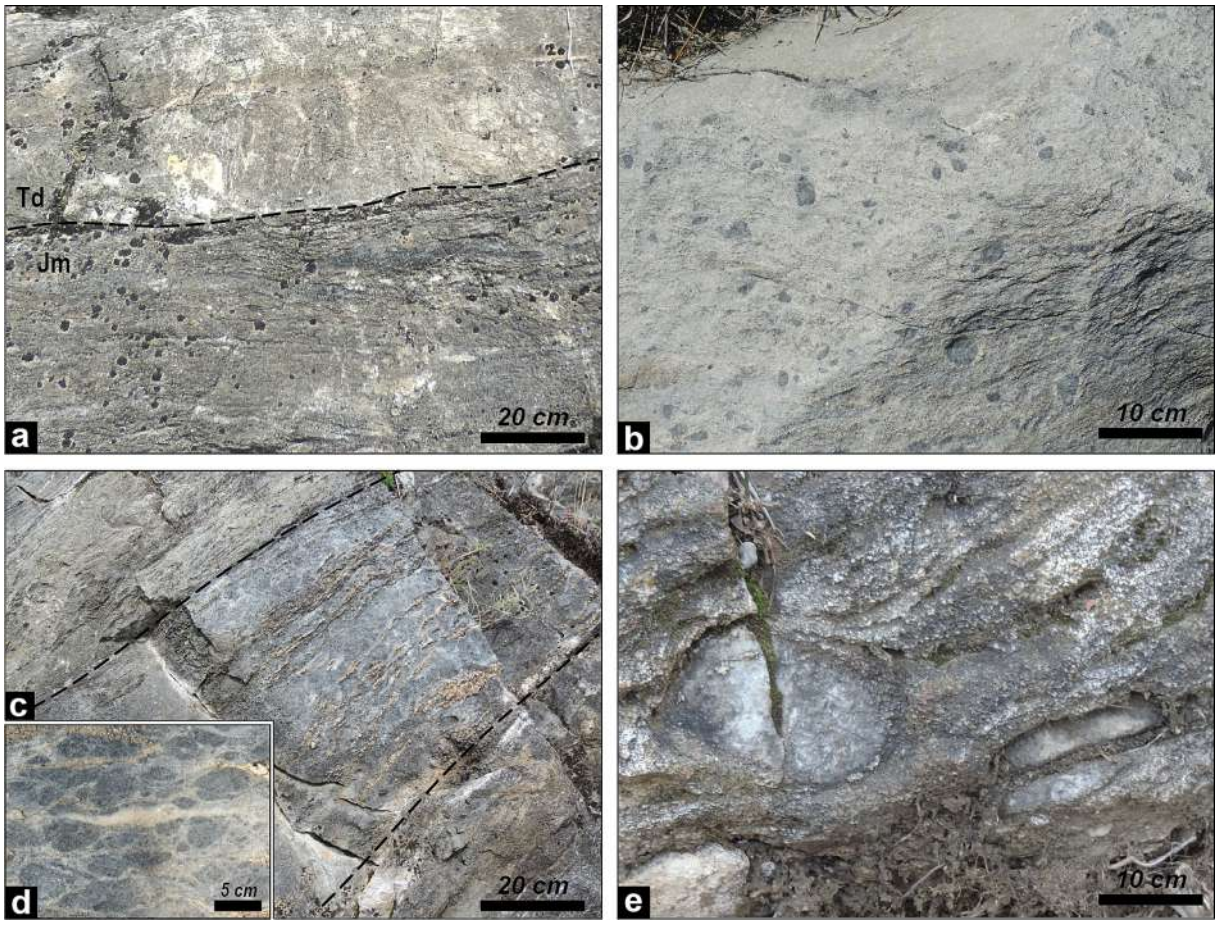

Fig. 6. Field images of the Jurassic lithostratigraphic units. (**a**) View of s contact (dashed black line) between the Triassic metadolostone (Td) and the Jurassic impure marble (Jm) (North of Foresto). (**b**) Close up view of a matrix-supported metabreccia showing bluish clasts embedded in a light grey quartz-carbonate matrix (close to Truc San Martino). (**c-d**) View of a clast-supported metabreccia interlayered (dashed black lines) within impure marble, and detail of the metabreccia layer (close to Truc San Martino). (**e**) Close up view of a matrix-supported metabreccia layer showing up to decimetre-sized clasts of the pre-rift metadolostone (close to C. Trucco).

imum age of deposition of their protolith. The two samples correspond to coarse-grained garnet- and chloritoid-bearing micaschists, and they are both characterized by the occurrence of several zircon crystals. These are quite inhomogeneous, varying from 50 to 500 μm in size and from sub-euhedral to sub-rounded in shape (Fig. 7a, b). The zircons crystals are characterized by complex internal structures, with different growth domains, and several cores show clear evidence of a multistage evolution. Oscillatory and sector zoning highlights that most of zircon crystals is of magmatic origin.

The analyses yield Th/U ratio varying from 0.04 to 1.89 (VS113) and from 0.09 to 2.14 (VS114). Measured zircons yield a large age span, from ca. 3 Ga to 500 Ma (VS113) and from ca. 2.7 Ga to 550 Ma (VS114). Zircon U-Pb age histograms and kernel density estimation (KDE) distributions were calculated (less than −15% and +5% discordance) and plotted by using IsoplotR (Vermeesch, 2018). Their age spectra distribution in both samples are characterized by the main age population at 500–700 Ma (age peak at 590–600 Ma) and two smaller age populations between 910–960 Ma and 1900–2100 Ma (Fig. 7c, d).

The youngest near-concordant zircon grains in both samples likely reflect Pb-loss and fluid-assisted recrystallization (Gasser at al., 2022), which may bias the Maximum Deposition Ages (MDA) estimates. To minimize this, more stringent discordance filters were applied. The MDAs for samples VS113 and VS114 are calculated by two methods that are the youngest grain function (Ludwig, 2003), based on $^{206}Pb/^{238}U$ ages with 3% discordance cut off, and the Maximum Likelihood Age (MLA), determined from radial plots with 5% discordance cut off (Vermeesch, 2021). The first method yields youngest grain ages of 481.67 + 15/−20 Ma and 530.21 + 13/−19 Ma for samples VS113 and VS114, respectively. The MLA is 490 ± 15 Ma (VS113) and 552.9 ± 6.4 Ma (VS114) (Fig. 7c, d). However, these youngest ages mainly result from zircon rims and it cannot be excluded that the true MDA may be older, such as is indicated by the main peak at ~ 600 Ma.

5.2. Borgone metagranite

Zircon crystals were separated from a sample of Borgone metagranite (VS77), in order to obtain its magmatic crystallization age. The sample corresponds to a coarse-grained and massive metagranite, and contains zircons crystals that are 100–200 μm sized and mainly sub-euhedral and rounded to elliptical in shape (Fig. 8a). Zircons are colourless to light violet in colour and larger crystals are characterized by voids and by apatite inclusions. They show well-developed sharp edges, and prismatic and bipyramidal shapes. Their medium aspect ratio is roughly homogeneous through the separated crystals, and only few zircon crystals show a lower aspect ratio, being tabular compared to the mains. The internal chemical texture is defined by an oscillatory growth zon-

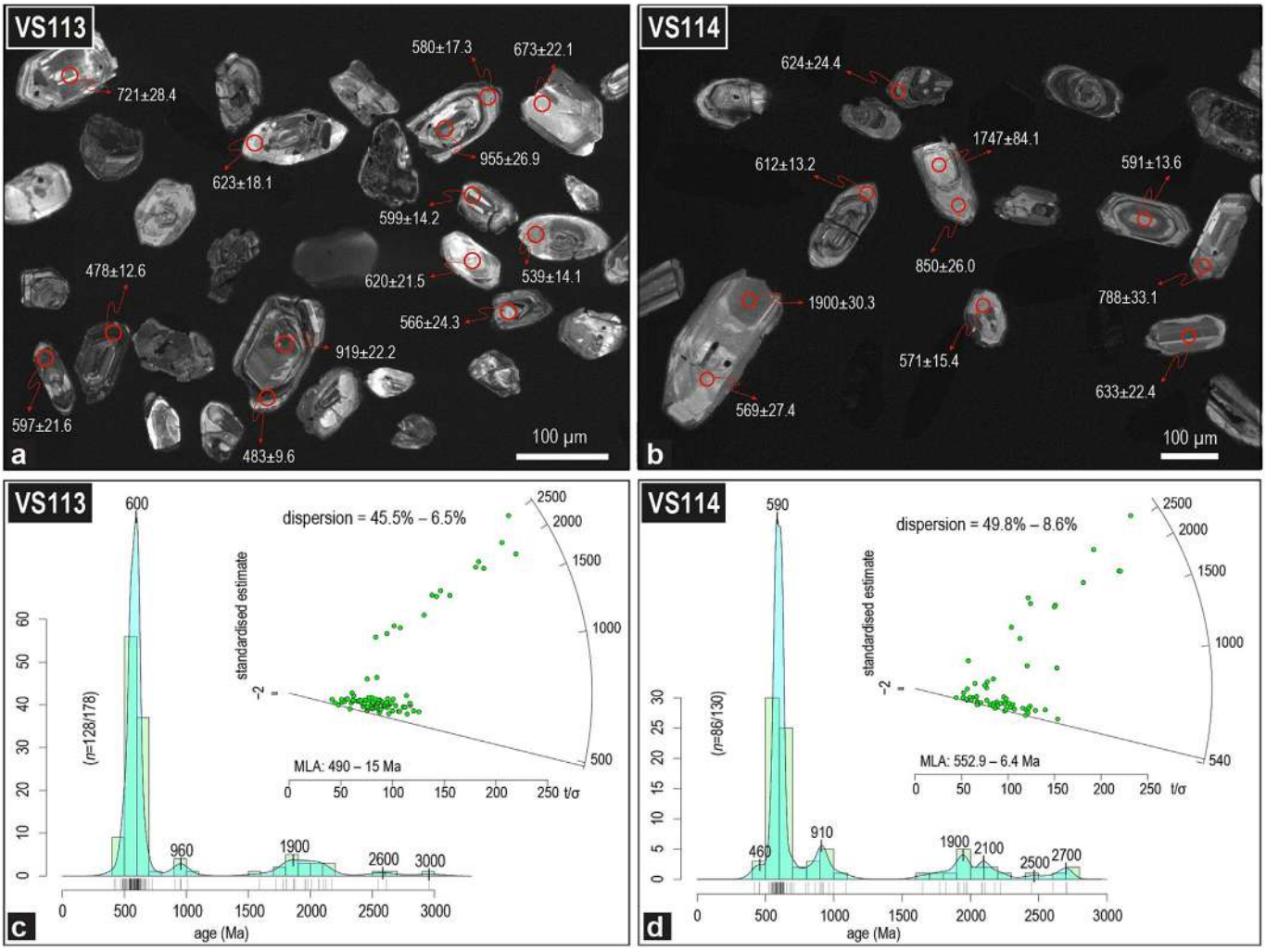

Fig. 7. U–Pb zircon geochronology of pre-Variscan micaschists (samples VS113 and VS114). (**a**–**b**) Representative images of analysed zircon grains (measured spots are shown by red circles with related ages in Ma), and (**c**–**d**) related detrital zircon ages distribution represented by Kernel Density Estimate and Maximum Likelihood Age plots.

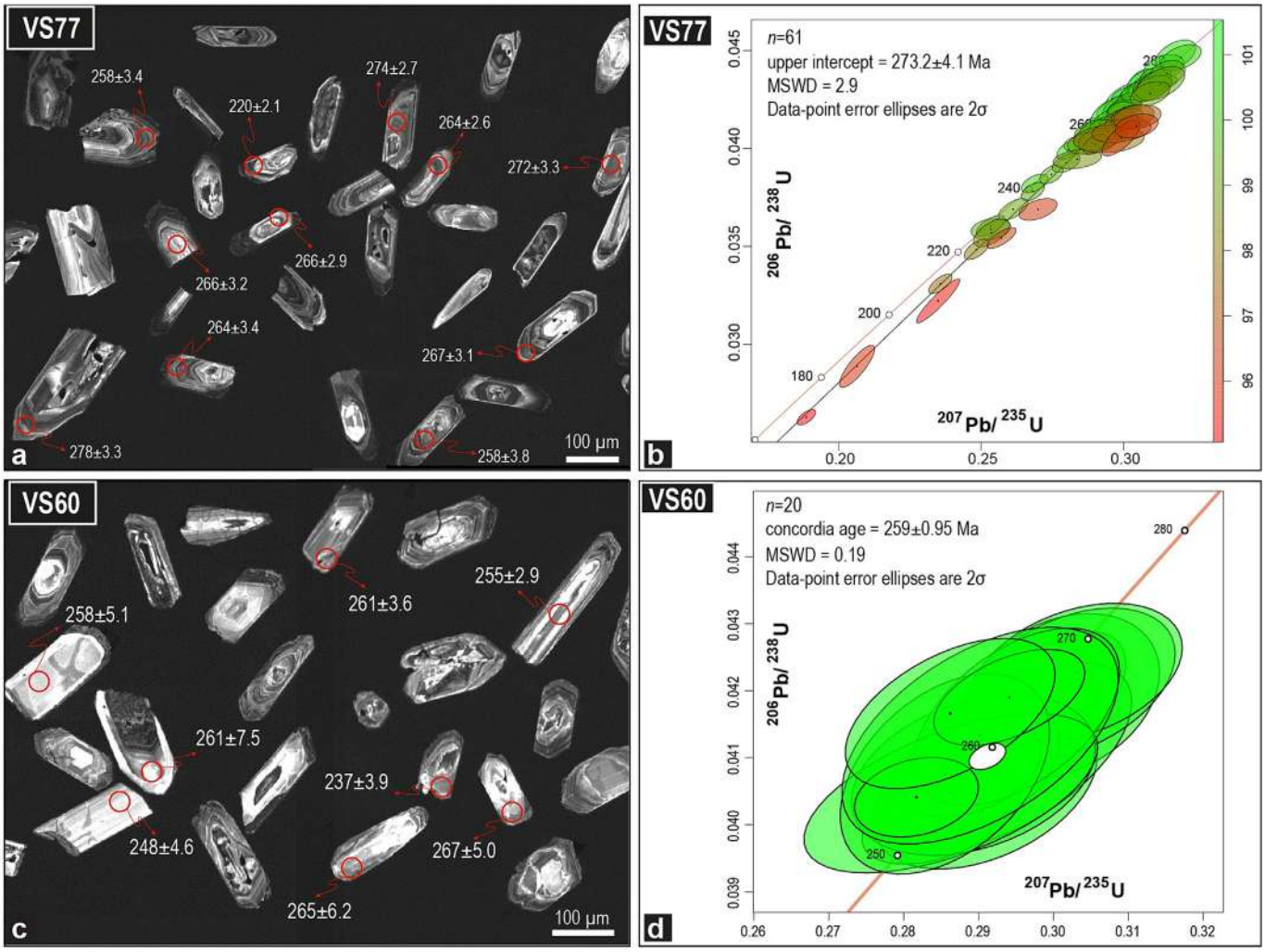

Fig. 8. U–Pb zircon geochronology of Borgone metagranite (sample VS77) and Luserna gneiss (sample VS60). (**a**, **c**) Representative images of analysed zircon grains (measured spots are shown by red circles with related ages in Ma), and **(b, d**) related Concordia plots.

ing, with broad bands locally organised in sectors. These features, together with the pristine morphology (i.e., sharp edges, not affected by erosion or detrital reworking), are typical of magmatic zircon growth. Some zircon grains also show complex internal structures, with altered and porous textures and patchy and convolute CL-zoning. This may be attributed to fluid-assisted dissolution and recrystallization of zircons (Rubatto, 2017; Zhou et al., 2023). Some other grains contain xenocryst cores.

Analyzed zircons are characterized by a Th/U ratio varying from 0.08 to 0.98 and yielded an age of 273.2 ± 4.1 Ma (MSWD = 2.9, *n* = 61), as upper intercept (<2% discordant) (Fig. 8b). Some few older ages obtained from xenocrysts, mostly ranging from ~ 350 Ma to 700 Ma, result from contamination of the host rock in the magma. Analytical points on oscillatory magmatic zoning also yield a spreading "tail" of younger ages, roughly spanning between 260 Ma and 230 Ma (Fig. 8b). The potential geological meaning of this "Concordia-parallel" Pb-loss is discussed further (Section 6.2).

5.3. Luserna augen gneiss

Zircon crystals were separated from a sample of Luserna augen gneiss (VS60), in order to obtain its magmatic crystallization age. The sample corresponds to a massive gneiss with porphyroclastic texture, and contains zircon crystals that are 100–300 µm sized and varying from euhedral to sub-euhedral (Fig. 8c). They are mainly few, pale-yellow to colourless and show well-developed sharp edges, and prismatic and bipyramidal shapes. Separated zircons are almost homogeneous in shape, with a high- to medium aspect ratio, and some few crystals are acicular in shape. The crystal internal chemical texture is mainly defined by oscillatory growth zoning. Some xenocryst cores inherited by the host rock also occur. The internal texture is locally altered, porous with patchy and convolute CL-zoning which may be attributed to fluid-assisted dissolution and recrystallization of zircons.

Analyzed zircons are characterized by a Th/U ratio varying from 0.11 to 0.84 and many analytical points are remarkably clustered. The analyses yield a Concordia age of 259 ± 0.95 Ma (MSWD = 0.19, *n* = 20; <1% discordant) (Fig. 8d). Some few older ages were obtained from xenocrysts and mostly range between ~ 590 Ma and 1200 Ma.

6. Discussion

The litostratigraphic data, integrated with geochemical and U-Pb geochronological results, constrain the pre-Alpine tectonostratigraphy of the northernmost sector of DMM (Figs. 2 and 3). It is the result of a long-lasting tectonostratigraphic and/or magmatic

evolution (Figs. 9a, 9b, 10a, 10b, 11a and 11b), during (i) pre-Permian, (ii) Permian, (iii) Triassic and (iv) Jurassic time intervals.

6.1. The pre-Permian tectonic evolution

The older rocks in the northernmost sector of DMM correspond to the pre-Variscan micaschist. Although these rocks lack pre-Alpine textural or mineralogical relicts, zircon ages spectra strongly suggest a polycyclic history. Notably, U-Pb geochronology shows no Carboniferous or Permian zircons, expected in monocyclic metasediments, but instead yields a main age population at 590–600 Ma, and subordintate peaks at 910–960 Ma and 1900–2100 Ma. The micaschists can thus be considered polycyclic, metamorphosed during both the Variscan and Alpine orogenic events. The abundance of zircon crystals suggests an origin from arenaceous sediments sourced from dismantling of an Ediacaran (Cadomian?) basement rich in Neoproterozoic magmatic rocks. Taking into account the results of the two methods applied for calculating the MDA, the protolith of the micaschist can be considered a sediment of Cambrian age. Comparable zircon populations have been documented in other DMM polycyclic metasediments (Manzotti et al., 2025b), intruded by Upper Ordovician granite (Bussy and Cadoppi, 1996; Nosenzo et al., 2024). This suggests that, at the time of intrusion, the micaschist protolith was already metamorphosed, and that youngest grain ages (480–490 Ma) may reflect rims formed during a Late Cambrian metamorphic event. Scattered metabasite bodies, likely emplaced as mafic dykes within the micaschist, further attest to a pre-Variscan age as suggested by their absence in the Borgone metagranite and Luserna gneiss, though their absolute age remain unknown.

Although pre-Variscan rocks of the northernmost DMM overall preserve few records of the Paleozoic history, comparison with other polycyclic metasediments described in the DMM and in the adjoining tectonic units helps reconstruct this history. Widespread evidence throughout the Alps points to erosion of an Ediacarian basement (Bertrand et al., 2000; Manzotti et al., 2015; Gilotti et al., 2023), particularly in the basement of the Briançonnais Zone (Thieblemont et al., 2023), where metasediments record a Late Cambrian metamorphic event. In the DMM, the scattered occurrence of pre-Variscan marble lenticular bodies interlayered within polycyclic micaschists (Groppo et al., 2007; Compagnoni et al., 2012; Cadoppi et al., 2016; Nosenzo et al., 2022), suggest deposition of predominantly siliciclastic sediments with minor limestones. Carbonate deposition during the Cambrian is consistent with successions across the Mediterranean (Cocco et al., 2023, and references therein) and in early Paleozoic terranes (Linnemann et al., 2007; Zak et al., 2025), and with the interpretation of the DMM as part of the northern Gondwana palaeomargin (von Raumer et al., 2013; Syahputra et al., 2023) (Fig. 1c).

In summary, after a possible Late Cambrian metamorphic event, the DMM pre-Variscan rocks were at least affected by (i) the Ordovician to Early Silurian magmatic event, widespread across the Alpine domains (Bergomi et al., 2017, and references therein), and (ii) the Late Devonian to Carboniferous subduction and collisional phases, related to the Variscan orogeny (Franke et al., 2020). The latter included an initial eclogite-facies metamorphic event (Rubatto et al., 2010; Maino et al., 2018), not documented in the DMM, followed by amphibolite-facies overprinting. Relicts of this metamorphic re-equilibration are locally preserved in the DMM and allow defining metamorphic conditions at P = 4–7 kbar and T = 500–650 °C, occurred at 324 Ma (Nosenzo et al., 2024). During the Variscan orogeny, the DMM was part of an upper crustal terrane involved in crustal thickening and, beginning around the Late Carboniferous period (304 Ma; Nosenzo et al., 2022), in the exhumation and post-collisional gravitational collapse of the belt.

6.2. The Permian magmatic event

Post-Variscan evolution in the northern DMM was characterized by Permian magmatism (Fig. 9a, b). U-Pb dating reveals an event lasting 15 Ma, with crystallization ages of ~ 274 Ma (Cisuralian-Guadalupian; Borgone metagranite) and 259 Ma (Guadalupian-Lopingian; Luserna gneiss). The Borgone metagranite represents a kilometre-scale pluton intruded into the pre-Variscan rocks. Geochemical studies highlight a sub-alkaline,

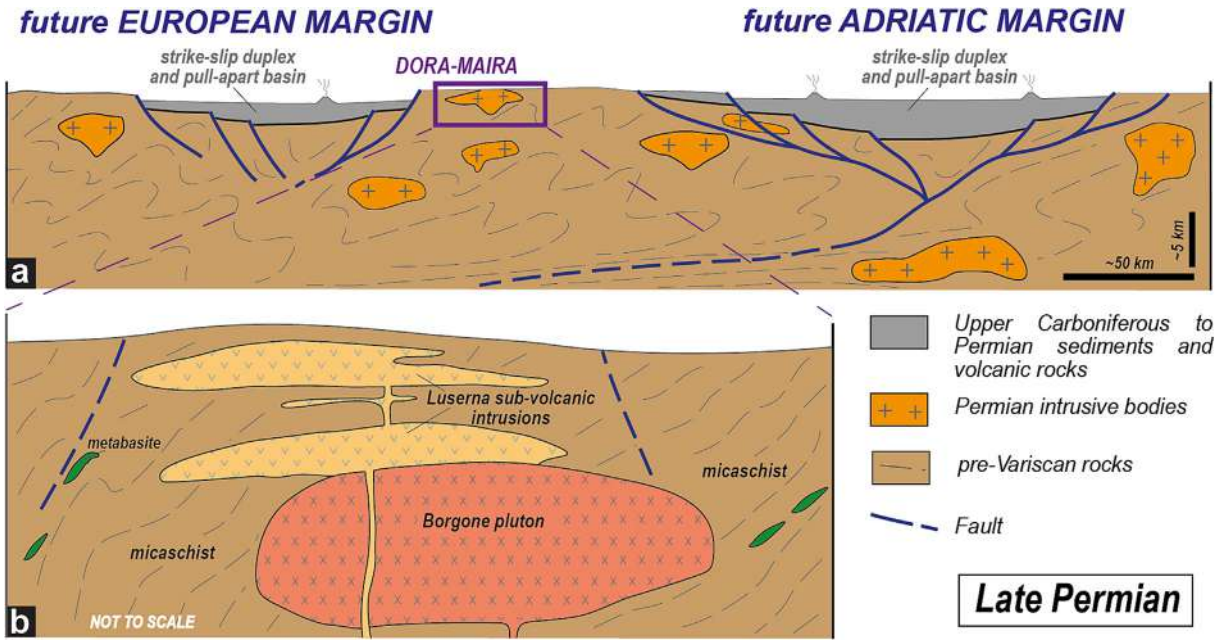

Fig. 9. (a) Schematic regional cross-section showing the tectonostratigraphic setting of the upper continental crust at Late Permian and the approximate location of the northern Dora-Maira Massif (modified from Decarlis et al., 2013; Ballèvre et al., 2018). (b) Late Permian tectonostratigraphy of the northernmost sector of the Dora-Maira Massif.

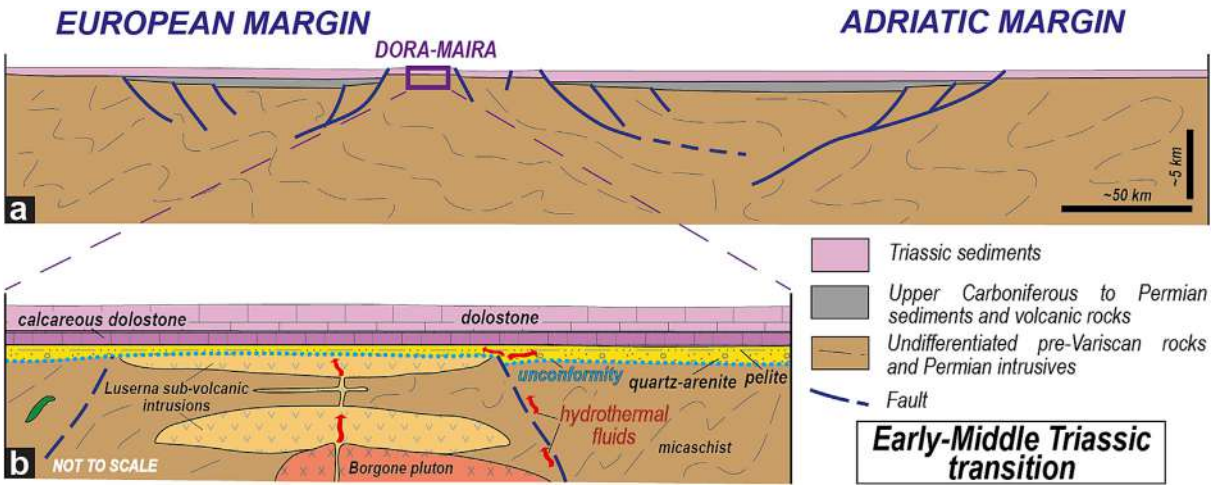

Fig. 10. (a) Schematic regional cross-section showing the pre-rift tectonostratigraphic setting at the Early-Middle Triassic transition, with the location of the northern Dora-Maira Massif (modified from Decarlis et al., 2013). (b) Early-Middle Triassic tectonostratigraphy of the northernmost sector of the Dora-Maira Massif.

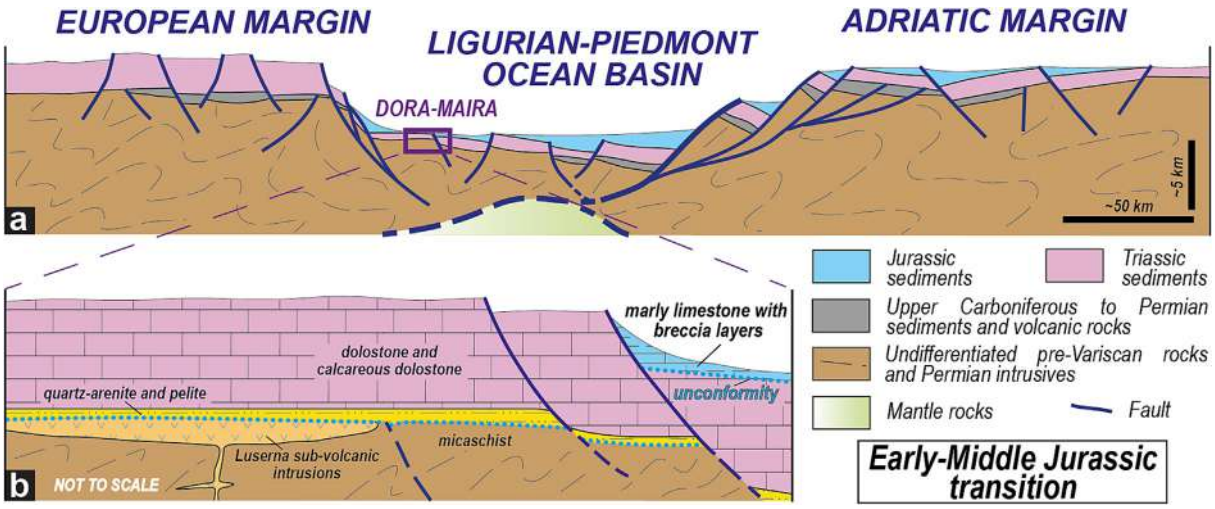

Fig. 11. (a) Schematic regional cross-section through the European and Adria margins and the (incipient) Ligurian-Piedmont Ocean Basin at the Early-Middle Jurassic transition, with the approximate location of the Dora-Maira Massif (modified from Mohn et al., 2012; Decarlis et al., 2013). (b) Syn-rift tectonostratigraphy of the northernmost sector of the Dora-Maira Massif.

slightly peraluminous composition, crystallized from an anatectic crustal melt at about 700 °C (Cadoppi, 1990). Differently from the Borgone metagranite, whose intrusive nature is also well constrained by the widespread occurrences of acidic dykes and mafic enclaves, the origin of the Luserna augen gneiss seems to be more complex. It differs from the Borgone metagranite not only for its younger age, but also for its stratigraphic occurrence and lithostratigraphic features. At the map scale (Fig. 2), the Luserna gneiss overlies both pre-Variscan rocks and the Borgone metagranite, and is structurally capped by the detached Mesozoic cover. The Luserna gneiss lacks differentiated dykes, and shows porphyroclastic texture and marked heterogeneity (massive vs. banded gneiss). The latter feature may also result from strain localization during Alpine deformation. However, the banded gneiss locally occurs as metres-thick horizon interlayered with the massive one, suggesting that its present-day fabric at least partly reflects primary heterogeneities of the protolith. Moreover, the banded gneiss is characterized by higher CIA values than the massive one, which are typical of weathered and possibly partially reworked magmatic rocks (Cruciani et al., 2013). The multiscale and diverse analytical data collectively suggest a subvolcanic origin for the Luserna augen gneiss. According to the nomenclature of volcanic rocks, the protolith of the massive gneiss would correspond to a porphyritic rhyolite, while the banded gneiss may derive from the weathering and/or reworking of the rhyolite itself (i.e., volcaniclastic rocks). Considering its stratigraphic setting, as well as the pronounced thickness variations and heterogeneity, the Luserna gneiss can be further interpreted as the product of multiple intrusions emplaced as laccoliths and sills (Fig. 9b) at shallow depths (i.e., from a few tens of metres up to three kilometres; Breitkreuz and Rocchi, 2018) within the pre-Variscan rocks.

The juxtaposition of the Luserna orthogneiss onto the Borgone metagranite suggests that this pluton was also emplaced at relatively shallow depth. Overall, the Permian magmatic bodies in the northernmost DMM can be interpreted as part of a shallow magmatic system. Vialon (1966) early suggested the existence of such a magmatic system, describing the occurrence of "*porphyroides granophyriques*" and "*porphyroides arcosiques*" in both the northern and southern DMM sectors. Granitoid rocks of Permian ages have been documented throughout the DMM (Bussy and Cadoppi, 1996; Gebauer et al., 1997), while occurrences of metavolcanic rocks are less frequently reported. However, rhyolitic

rocks have been locally identified (Balestro et al., 2022a; Nosenzo et al., 2024). The crystallization of the different DMM intrusive bodies appears to follow a distinct trend, with older (~280–300 Ma) and younger (~270–260 Ma) ages obtained from magmatic rocks located in the tectonically lower unit (i.e., the blueschist-facies Pinerolo Unit) and in the upper eclogite-facies units, respectively. These two age groups have been referred to two distinct magmatic suites, roughly reflecting a progressive evolution from calc-alkaline to more alkaline melts (Bussy and Cadoppi, 1996). This evolutionary trend has also been recognized in other sectors of the Western Alps (i.e., the first and second magmatic cycles of Cortesogno et al. (1998)) and may be linked with a tectonic shift from widespread Early Permian strike-slip regimes to Late Permian extensional tectonics (Sandrone et al., 1993; Spalla et al., 2014; Festa et al., 2020). During the Permian time, the northernmost DMM may have represented a structural high controlled by active tectonics (Fig. 9a, b), as suggested by the absence of upper Carboniferous to Permian metasediments found in other DMM sectors (Manzotti et al., 2016; Balestro et al., 2022a) and deposited in low elevation areas. It is worth noting that the northernmost DMM sector was only affected by the later phases of the broader magmatic event that spanned from Late Carboniferous to the Permian, widely described across the Western Alps (Ballèvre et al., 2018, and references therein) and adjoining areas (e.g., Casini et al., 2015). Unlike the basement of the Briançonnais Zone, where volcanic activity was more prominent, the DMM is characterized primarily by the emplacement of intrusive and subvolcanic bodies during the Permian magmatic episode.

In the northernmost DMM, hydrothermal processes also marked the Permian magmatic event. These processes followed the emplacement of the Borgone metagranite and Luserna orthogneiss and are evidenced by the occurrence of pre-Alpine quartz veins, more common in the Luserna gneiss but also present in the Borgone metagranite and pre-Variscan micaschist. Emplacement of quartz veins was locally associated with minor mineralizations, as highlighted by the Fe-Mn oxides-rich layers found in the Lower Triassic quartzite (i.e., the former basement-cover transition, see below). Additional evidence of hydrothermal activities includes relicts of saddle-dolomite crystals within the marble at the base of the Middle to Upper Triassic cover succession. The occurrence of saddle-dolomite has been related to precipitation from low temperature magmatic fluids (Diamanti et al., 2024). Fluid circulation is further revealed by the occurrence, just outside the study area (i.e., the southern side of the Susa Valley), of tourmaline-rich leucogneiss, which crystallized from highly differentiated boron-enriched residual melts (Cadoppi, 1990; Sandrone et al., 1993). The ascent of hydrothermal fluids was likely driven by extensional –faults (Fig. 10b). These findings suggest a hydrothermal event spanning at least from the latest Permian period to the end of the Early Triassic. Further potential evidence for prolongated hydrothermalism lies in the "tail" of younger ages, roughly between 260 Ma and 230 Ma, obtained from the Borgone metagranite. This "Concordia-parallel" Pb-loss, resulted after partial zircon resetting, may reflect weathering of the original granite during the hydrothermal event, though further studies are needed to confirm this. Similar age "tails", spanning approximatively 260 Ma and 210 Ma, have been observed in Permian metagranites and metavolcanic rocks in the southern DMM (Gebauer et al., 1997) and in the Ligurian Briançonnais basement (Dalla Giovanna et al., 2009), respectively. In both cases, the partial resetting of zircon has been attributed to a regional-scale thermal perturbation associated with the onset of the rifting phase. However, localized hydrothermal effects, such as those documented in other Permian metagranites of the Western Alps (Luisier et al., 2021), cannot be ruled out.

6.3. The Triassic and Jurassic tectonostratigraphic evolution

The complex setting inherited from the pre-Permian tectonostratigraphic and tectonometamorphic evolution culminated in the Permian magmatic event. The sub-sequent Triassic evolution marks the transition to the Early – Middle Jurassic rifting stage (Figs. 10a, b). Although extensional events (i.e., earlier minor rifting stages) are documented during the Middle to Late Triassic period (e.g., Marroni and Pandolfi, 2007; Berra et al., 2009; Mohn et al., 2012; Masini et al., 2013; Marroni et al., 2017), in the following, we use the terms "pre-rift" and "*syn*-rift" succession in reference to the main rifting event, which occurred in the Early to Middle Jurassic period, and led to the opening of the Ligurian-Piedmont Ocean Basin.

6.3.1. The Triassic tectonostratigraphic evolution

Above the Paleozoic basement, the Lower Triassic succession consists of a heterogeneous stratigraphic sequence made up of paragneiss, quartzite, quartz-rich schist and carbonate-bearing micaschist. The paragneiss is characterized by K-feldspar porphyroclasts and quartz aggregates, representing relicts of clastic textures. The latter are better preserved in the southern side of the Susa Valley), where metasandstone with clasts of quartz and K-feldspar porphyroclasts (i.e., the Rodetti paragneiss) and metaconglomerate with decimetre-sized metagranite clasts (i.e., the Monte Muretto metaconglomerate) have been described (Pognante, 1980; Cadoppi et al., 2002; Ghignone et al., 2020). The paragneiss is associated with quartzite, which is locally enriched in Fe-Mn oxides and derives from quartz-arenites with minor phyllosilicates and feldspars. These metasediments reflect erosion of the Paleozoic basement and tectonic uplift likely controlled by active tectonics (Fig. 10b). The varying thickness of this heterogeneous Lower Triassic succession, indirectly suggests the deposition over an articulated basement and/or a fault-controlled depositional setting. Although Alpine deformation and metamorphic recrystallization prevent the identification of primary faults, this scenario aligns well with observations from other sector of the Internal Western Alps (e.g., the Canavese Zone), where the time of fault activity is well-constrained to Early-Middle Triassic time (see Festa et al., 2020; Balestro et al., 2022b). Deposition occurred in alluvial-deltaic to shoreface settings, comparable to the Ponte di Nava Quartzite in the Briançonnais cover successions, which overlie Verrucano-like metasediments (Decarlis et al., 2013; Bertok et al., 2018; Costamagna, 2024) and have been referred to the Olenekian Stage based on local vertebrate footprints (Petti et al., 2020). The clastic component was sourced from nearby rocks, corresponding to the Borgone metagranite and Luserna gneiss, and possibly the uppermost pre-Variscan units involved in dismantling processes. Above the quartzite, a few meters of quartz-rich schist and carbonate-bearing micaschist occurs, interpreted as derived from a ± calcareous pelite protolith. The grain size and the possible occurrence of primary Fe-carbonate suggests a correlation with the Val Marenca Pelites (Vanossi, 1974), which locally overlie the Ponte di Nava Quartzite. These pelites deposited in a lagoon setting during the Anisian stage as indicated by Chirotheriid footprints (Santi et al., 2015). These Lower Triassic metasediments are scattered in the northern sector of DMM (Cadoppi and Tallone, 1992; Balestro et al., 2011) but more abundant to the south (i.e., the Sampeyre *Ensemble* of Vialon (1966)). In the northernmost DMM, due to strain localization along the basement-cover transition, their thickness cannot be defined in detail but it roughly does not exceed few tens of metres, whereas in the Briançonnais successions they range from ~ 100 m (External Briançonnais units) to ~ 250 m (Internal Briançonnais units), including the Verrucano-like clastic rocks (Decarlis et al., 2013; d'Atri et al., 2016). Comparable reduced thickness occurs in other Internal Crystalline Massifs (Elter, 1972;

Keller and Schmid, 2001) and in more internal units of the Gran St-Bernard Nappe System (Pantet et al., 2020). These variations suggest the occurrence within the Briançonnais realm and adjoining areas, wherein the DMM continental crust was localized, of fault-banded blocks characterized by different subsidence rates (Fig. 10a).

The succession continued upward with a carbonate rocks succession (Fig. 10b). The basal few metres consist of banded marble and dolomitic marble overlain by thick metadolostone. Banded marble locally contains relicts of saddle-dolomite crystals, whereas dolomitic marble shows calcite in microscale aggregates interpreted as cement filling original shrinkage pores. These rocks derive from limestone and calcareous dolostone, consisting of calcite and dolomite with very minor quartz and phyllosilicates. Overall, this pre-rift succession is characterized by a stratigraphically upward decrease in the pelite component of their original sediments. The overlying metadolostone ranges from whitish and homogeneous in the lower part to well-bedded and more colour-variegated higher up. Difference in trace elements content (Fe, Mn and Sr) and in the isotopic ratios of carbon and oxygen, further support the occurrence of different types of metadolostone (Agostoni et al., 2017). These rocks were very early dolomitized (Gambino et al., 2019), and have been regionally considered Middle to Late Triassic in age.

Remnants of evaporitic facies, which are widespread in the Briançonnais successions (Michard et al., 2004; Barré et al., 2020), are absent in the DMM. Instead, the marble and metadolostone document a carbonate platform depositional setting (Fig. 10b), and, at least for some intervals (i.e., the ones showing remnants of shrinkage pores), a peritidal flat depositional environment can be inferred. The marble and metadolostone can be correlated with the Anisian Costa Losera (Lualdi and Bianchi, 1990), the Ladinian San Pietro dei Monti Dolostone (Vanossi, 1969), and the Carnian – Norian Monte Arena Dolostone (Boni et al., 1971). Not all these Formations are present in the Briançonnais successions (i.e., the Internal and External Briançonnais gap *Auct.*). However, they characterize the pre-Piedmont domain (i.e., the transition zone between the European distal margin and the Ligurian-Piedmont Ocean Basin; Balestro et al., 2022a; Michard et al., 2022). In particular, the occurrence of the Monte Arena Dolostone is thought to record deposition associated with an extensional stage, interpreted as the first minor Middle-Late Triassic rifting stage (see Decarlis et al., 2013 for details). Unlike Briançonnais successions, the DMM carbonate succession does not record Late Triassic–Early Jurassic uplift and karstification (Fig. 10a) (Faure and Mégard-Galli, 1988; Tricart et al., 1988; Decarlis et al., 2008). Instead, it resembles the pre-Piedmont succession (Michard, 1967) and the Valle Maira-type succession (Ballèvre et al., 2020), although with reduced thickness (~100 m compared to ~1 km), possibly modified by both Jurassic and Alpine tectonics. The characteristics of the Middle-Late Triassic succession of the DMM, thus suggest that deposition occurred during a persistent extensional stretching of the European continental crust, likely driven by pure shear-dominated extension as documented in other sectors of the Alpine-Apennine system (see, e.g., Mohn et al., 2012; Masini et al., 2013; Marroni et al., 2017). Crustal stretching persisted into the Early Jurassic period with the onset of the main rifting event, which led to the opening of the Ligurian-Piedmont Ocean Basin, as described in the following.

6.3.2. The Early-Middle Jurassic rifting event

The Mesozoic cover succession closes upward with a ten of meters thick succession of impure marble and calcschist, overlying the metadolostone. These rocks derive from marly limestone and are interlayered by two types of metabreccia horizons. The first type derives from intraclastic breccia layers, sourced from erosion and reworking of early cemented calcareous beds, and they were also found in other sectors of the DMM (Michard, 1967; Nosenzo et al., 2024). Notably, this metabreccia is very similar to the pseudonodular layers described in the Middle Jurassic Rio di Nava Limestone in Briançonnais cover successions, and interpreted as *syn*-rift seismites (Bertok et al., 2011). The latter formed after seismic shocks that triggered fluidization of unconsolidated beds and rupture of the cemented ones, and it clearly indicates the occurrence of active faults (Fig. 11b). The second type of metabreccia horizons, characterized by the occurrence of metadolostone clasts, indicates synsedimentary reworking of dolomitic material sourced from the carbonate platform and deposited along tectonically active escarpments. Similar metabreccia occurs in the Middle Jurassic Monte Galero Breccia in the pre-Piedmont successions (Michard, 1967; Dumont, 1984; Decarlis et al., 2013), and in internal units of Gran St-Bernard Nappe System (i.e., Evoléne Series; Pantet et al., 2020). Such a tectonostratigraphic setting marks the onset of rifting phase and margin segmentation related to the opening of the Ligurian-Piedmont Ocean Basin (e.g., Handy et al., 2010; Balestro et al., 2018; Ribes et al., 2019). The impure marble, calcschist and metabreccia are therefore interpreted as remnants of the *syn*-rift succession of northern DMM (Fig. 11a, b). These *syn*-rift metasediments are notably thinner in the study area compared to those occurring in the pre-Piedmont succession, but it may be an apparent thinning, not reflecting the original depositional thickness. It is plausible that a significant portion of the *syn*-rift succession was tectonically excised, as also suggested by the nearly absence of post-rift (Late Jurassic to Cretaceous) metasediments. Cretaceous calcschist (Marthaler et al., 1986) occurs only within the Foresto Shear Zone (i.e., the shear zone separating the DMM from the overlying Susa and Lanzo valleys *meta*-ophiolites; Balestro et al., 2025a), and, due to the strong deformation overprint, its origin is unclear.

The *syn*-rift succession of the northernmost DMM was deposited during regional extensional to transtensional tectonics associated with the Jurassic opening of the Ligurian-Piedmont Ocean Basin (Lemoine et al., 1986; Handy et al., 2010; Frasca et al., 2024). In this tectonic frame, the DMM continental crust would have been located near the main break-up zone (Fig. 11a), likely involving hyper-extension of the passive margin with consequent formation of crustal allochthonous. This Jurassic tectonic evolution is indirectly supported by metamorphic peaks ages of ~60 Ma recorded in the northern DMM (Manzotti et al., 2025a). These ages are significantly older than those from the southern DMM (~35–40 Ma; Bonnet et al., 2022, and references therein), and are comparable to/or slightly older than ages obtained from subducted oceanic rocks (Agard, 2021, and references therein). This suggests that during Alpine orogeny portions of the DMM continental crust were subducted alongside oceanic lithosphere, pointing to a close spatial and temporal relationship between the two domains. The potential localization of DMM along a hyperextended Jurassic palaeomargin, or within a transitional zone between the Briançonnais domain and the Ligurian-Piedmont Ocean Basin, is further suggested by the local occurrence of mantle rocks within it (Henry et al., 1993; Balestro et al., 2020). Earlier models had alternatively proposed intra-oceanic (Platt, 1986; Dal Piaz, 1999) or Adria-facing (Platt, 1986; Polino et al., 1990) paleogeographic positions for the Internal Crystalline Massifs (i.e., DMM, Gran Paradiso and Monte Rosa). In this framework, *syn*-rift extensional tectonics and crustal hyperextension likely contributed to the stretching and thinning of the pre-rift successions within the DMM. Analogous tectonic processes have been documented in the Adria-derived Canavese Zone (Barale et al., 2021; Balestro et al., 2022b), where Jurassic hyperextension of the distal margin (Ferrando et al., 2004) has been linked to the reactivation of Permian structural inheritance (Festa et al., 2020). It is important to note that, unlike the Adria paleomargin

and its extensional allochthons (Beltrando et al., 2014), lower crustal rocks have not currently been documented within the DMM. This absence may reflect the effects of an asymmetrical rift system (Lemoine et al., 1987; Marroni and Pandolfi, 2007) and mechanical decoupling between upper and lower crustal levels during extension (Ballèvre et al., 2020).

7. Conclusions

Our new lithostratigraphic and geochronological data from the northern DDM provide a refined record of the Paleozoic to Mesozoic evolution of the European distal margin prior to Alpine convergence. Although intense Alpine metamorphic and tectonic overprinting, detailed geological mapping and U–Pb geochronology reveal a multistage pre-orogenic evolution that links the Gondwana inheritance to Alpine paleogeography.

The pre-Variscan micaschists record Cambrian metasediments derived from erosion of a Neoproterozoic–Paleoproterozoic source region along the northern Gondwana margin. Their polycyclic history, involving Ordovician–Silurian magmatism, and Devonian–Carboniferous subduction and collision, formed a heterogeneous basement architecture later reactivated during Permian and Alpine tectonics. U–Pb dating constrains emplacement of the Borgone metagranite (~274 Ma) and the Luserna gneiss (~259 Ma), which together document a shallow magmatic system linked to lithospheric thinning and a regional transition from post-Variscan strike-slip tectonics to Late Permian-Early Triassic extension. Associated hydrothermal activity extended into the Early Triassic, marking the onset of crustal destabilization. During the Mesozoic, the basement was unconformably overlain by quartz-rich arenites, pelites, and Triassic carbonates (i.e., present-day paragneisses, quartzites, carbonate micaschists, marbles and metadolostones), recording progressive marine transgression and carbonate platform growth. An early, minor, rifting stage characterized the DMM during the Middle-Late Triassic period. Late Lower Jurassic to Middle Jurassic *syn*-rift metasediments (i.e., impure marbles, calcschists and metabreccias) document extensional tectonics associated with the main rifting stage, which led to the opening of the Ligurian–Piedmont Ocean Basin.

Taken together, these results show that the DMM preserves an inherited tectonostratigraphic archive that strongly influenced the Alpine cycle from rifting to subduction. The early subduction of the northern DMM (~60 Ma), compared to southern sectors, indicates its location within a transitional paleogeographic domain between Briançonnais realm and Ligurian–Piedmont Ocean Basin, and implies that the paleogeographic position of the DMM cannot simply be referred to as the distal part of the Briançonnais microcontinent (Schmid et al., 2004). This highlights the role of pre-rift architecture in controlling paleogeography and in governing the sequence of geodynamic processes (i.e., rift, drift, subduction, and collision) that constructed the Western Alps. Successive cycles of sedimentation, magmatism, and rifting could have created structural and rheological heterogeneities, influencing strain localization and diachronous subduction of continental fragments. These results not only sharpen paleogeographic reconstructions of the Western Alps but also highlight how deep-time inheritance fundamentally influences the architecture and mechanical behaviour of collisional orogens worldwide.

CRediT authorship contribution statement

Gianni Balestro: Writing – original draft, Validation, Supervision, Methodology, Investigation, Funding acquisition, Formal analysis, Data curation, Conceptualization. **Matthieu Roà:** Writing – original draft, Validation, Methodology, Investigation, Formal analysis, Data curation, Conceptualization. **Carlo Bertok:** Writing – original draft, Validation, Methodology, Investigation, Formal analysis, Data curation, Conceptualization. **Marco Gattiglio:** Writing – review & editing, Validation, Methodology, Investigation, Formal analysis, Data curation, Conceptualization. **Stefano Ghignone:** Writing – review & editing, Validation, Methodology, Investigation, Formal analysis, Data curation, Conceptualization. **Chiara Groppo:** Writing – original draft, Visualization, Methodology, Investigation, Formal analysis, Data curation, Conceptualization. **Valby van Schijndel:** Writing – original draft, Visualization, Methodology, Investigation, Formal analysis, Data curation, Conceptualization. **Andrea Festa:** Writing – original draft, Validation, Methodology, Investigation, Funding acquisition, Formal analysis, Data curation, Conceptualization.

Declaration of competing interest

The authors declare that they have no known competing financial interests or personal relationships that could have appeared to influence the work reported in this paper.

Acknowledgments

Many thanks are due to A. Borghi for his important contribution in geochronological analyses and discussion about the geology of the Dora-Maira Massif. L. Martire is greatly acknowledged for sharing his experience in cathodoluminescence analyses. We extend our sincere thanks to the Handling Editor S. Kwon and to two anonymous reviewers for their constructive and thorough reviews. This work was supported by research grants from the Italian Ministry of University and Research (Cofin-PRIN 2020 'POEM project – POligEnetic Melanges: anatomy, significance and societal impact': grant No. 2020542ET7_003 awarded to A.F.).

References

Agard, P., 2021. Subduction of oceanic lithosphere in the Alps: Selective and archetypal from (slow- spreading) oceans. Earth Sci. Rev. 214, 103517.

Agostoni, A., Barello, F., Borghi, A., Compagnoni, R., 2017. The white marble of the Arch of Augustus (Susa, North-Western Italy): Mineralogical and petrographic analysis for the definition of its origin. Archaeometry 59 (3), 395–416.

Avigad, D., Chopin, C., Le Bayon, R., 2003. Thrusting and extension in the southern Dora-Maira ultra-high pressure massif (Western Alps): View from below the coesite-bearing unit. J. Geol. 111 (1), 57–70. https://doi.org/10.1086/344664.

Balestro, G., Fioraso, G., Lombardo, B., 2011. Geological map of the upper Pellice Valley (Italian Western Alps). J. Maps 7 (1), 634–654. https://doi.org/10.4113/jom.2011.1213.

Balestro, G., Fioraso, G., Lombardo, B., 2013. Geological map of the Monviso massif (Western Alps). J. Maps 9 (4), 623–634. https://doi.org/10.1080/17445647.2013.842507.

Balestro, G., Festa, A., Dilek, Y., Tartarotti, P., 2015. Pre- Alpine extensional tectonics of a peridotite localized oceanic core complex in the late Jurassic, high-pressure Monviso ophiolite (Western Alps). Episodes 38 (4), 266–282 https://doi.org/10.18814/epiiugs/2015/v38i4/82421.

Balestro, G., Festa, A., Borghi, A., Castelli, D., Gattiglio, M., Tartarotti, P., 2018. Role of late Jurassic intra-oceanic structural inheritance in the Alpine tectonic evolution of the Monviso meta-ophiolite complex (Western Alps). Geol. Mag. 155 (2), 233–249.

Balestro, G., Festa, A., Dilek, Y., 2019. Structural architecture of the Western Alpine Ophiolites, and the Jurassic seafloor spreading tectonics of the Alpine Tethys. J. Geol. Soc. London 176 (5), 913–930. https://doi.org/10.1144/jgs2018-099.

Balestro, G., Nosenzo, F., Cadoppi, P., Fioraso, G., Groppo, C., Festa, A., 2020. Geology of the southern Dora- Maira Massif: Insights from a sector with mixed ophiolitic and continental rocks (Valmala tectonic unit, Western Alps). J. Maps 16 (2), 736–744. https://doi.org/10.1080/17445647.2020.1824825.

Balestro, G., Festa, A., Cadoppi, P., Groppo, C., Roà, M., 2022a. Pre-orogenic tectonostratigraphic evolution of the European distal margin-alpine Tethys transition zone in high-pressure units of the southwestern Alps. Geosciences 12 (10), 358. https://doi.org/10.3390/geosciences12100358.

Balestro, G., Festa, A., De Caroli, S., Barbero, E., Borghi, A., Gianotti, F., 2022b. Multistage tectono-stratigraphic evolution of the Canavese Intracontinental Suture Zone: new constraints on the tectonics of the Inner Western Alps. Geosci. Front. 13 (6), 101448. https://doi.org/10.1016/j.gsf.2022.101448.

Balestro, G., Gattiglio, M., Roà, M., Festa, A., 2025a. Tectonic relationships between the Paleozoic basement and the Mesozoic cover succession in the northern Dora-Maira Massif (Susa Valley, Western Alps). J. Maps 21 (1), 2451785. https://doi.org/10.1080/17445647.2025.2451785.

Balestro, G., van Schijndel, V., Gattiglio, M., Borghi, A., Ghignone, S., 2025b. Laser ablation inductively coupled mass spectrometry (LA-ICP-MS) of zircon U-Pb from a European terrane (Western Alps, Italy). GFZ Data Services. https://doi.org/10.5880/fidgeo.2025.061.

Ballèvre, M., Manzotti, P., Dal Piaz, G.V., 2018. Pre- Alpine (Variscan) inheritance: a key for the location of the future Valaisan Basin (Western Alps). Tectonics 37 (3), 786–817. https://doi.org/10.1002/2017TC004633.

Ballèvre, M., Camonin, A., Manzotti, P., Poujol, M., 2020. A step towards unraveling the paleogeographic attribution of pre-Mesozoic basement complexes in the Western Alps based on U-Pb geochronology of Permian magmatism. Swiss J. Geosci. 113, 12.

Barale, L., Bertok, C., d'Atri, A., Mantovani, A., Martire, L., Agostini, S., Bernasconi, S., Gerdes, A., Ferrando, S., 2021. Syn-rift hydrothermal circulation in the Mesozoic carbonates of the western Adriatic continental palaeomargin (Western Southalpine Domain, NW Italy). Basin Res. 33, 3045–3076. https://doi.org/10.1111/bre.12594.

Barré, G., Strzerzynski, P., Michels, R., Guillot, S., Cartigny, P., Thomassot, E., Lorgeoux, C., Assayag, N., Truche, L., 2020. Tectono-metamorphic evolution of an evaporitic décollement as recorded by mineral and fluid geochemistry: the "Nappe des Gypses" (Western Alps) case study. Lithos 358–359, 105419. https://doi.org/10.1016/j.lithos.2020.105419.

Beltrando, M., Compagnoni, R., Lombardo, B., 2010. (Ultra-) High-pressure metamorphism and orogenesis: an Alpine perspective. Gondwana Res. 18 (1), 147–166.

Beltrando, M., Manatschal, G., Mohn, G., Dal Piaz, G., Vitale, B.A., Masini, E., 2014. Recognizing remnants of magma-poor rifted margins in high-pressure orogenic belts: the Alpine case study. Earth Sci. Rev. 131, 88–115. https://doi.org/10.1016/j.earscirev.2014.01.001.

Berra, F., Galli, M.T.M., Reghellin, F., Torricelli, S., Fantoni, R., 2009. Stratigraphic evolution of the Triassic-Jurassic succession in the Western Southern Alps (Italy): the record of the two-stage rifting of the distal passive margin of Adria. Basin Res. 21 (3), 335–353.

Bergomi, M.A., Dal Piaz, G.V., Malusà, M.G., Monopoli, B., Tunesi, A., 2017. The grand St Bernard-Briançonnais nappe system and the paleozoic inheritance of the western alps unraveled by zircon U-Pb dating. Tectonics 36 (12), 2950–2972.

Bertok, C., Martire, L., Perotti, E., d'Atri, A., Piana, F., 2011. Middle-late Jurassic syndepositional tectonics recorded in the Ligurian Briançonnais succession (Marguareis–Mongioie area, Ligurian Alps, NW Italy). Swiss J. Geosci. 104 (2), 237–255.

Bertok, C., Musso, A., d'Atri, A., Martire, L., Piana, F., 2018. Geology of the Colle di Tenda – Monte Marguareis area (Ligurian Alps, NW Italy). J. Maps 14 (2), 542–551. https://doi.org/10.1080/17445647.2018.1500497.

Bertrand, J.M., Pidgeon, R.T., Leterrier, J., Guillot, F., Gasquet, D., Gattiglio, M., 2000. SHRIMP and IDTIMS U-Pb zircon ages of the pre-Alpine basement in the Internal Western Alps (Savoy and Piemont). Schweiz. Mineral. Petrogr. Mitt. 80 (3), 225–248.

Boni, A., Cerro, A., Gianotti, R., Vanossi, M., 1971. Note Illustrative della Carta Geologica d'Italia alla scala 1:100000, Foglio 92-93, Albenga-Savona. Serv. Geol. It., 142 (in Italian)

Bonioli, L., Cadoppi, P., Sacchi, R., 1992. Occurrence of metavolcanics in the southernmost Dora-Maira Massif (Italian Western Alps). In: Carmignani, L., Sassi, F.P. (Eds.), Contributions to the Geology of Italy with Special Regard to the Paleozoic Basements. A volume dedicated to Tommaso Cocozza. IGCP Proj. 276. Newsletter (5), 237–240.

Bonnet, G., Chopin, C., Locatelli, M., Kyander-Clark, A., Hacker, B.R., 2022. Protracted subduction of the European hyperextended margin revealed by rutile U- Pb geochronology across the Dora-Maira massif (W. Alps). Tectonics 41 (4), e2021TC007170. https://doi.org/10.1029/2021TC007170.

Borghi, A., Cadoppi, P., Porro, A., Sacchi, R., Sandrone, R., 1984. Osservazioni geologiche nella Val Germanasca e nella media Val Chisone (Alpi Cozie). Boll. Mus. Sci. Nat. Torino 2, 503–530 (in Italian).

Breitkreuz, C., Rocchi, S., 2018. Physical Geology of Shallow Magmatic Systems: Dykes, Sills and Laccoliths. Springer, 409 pp. https://doi.org/10.1007/978-3-319-14084-1.

Bussy, F., Cadoppi, P., 1996. U–Pb zircon dating of granitoids from the Dora-Maira massif (Western Italian Alps). Schweiz. Mineral. Petrogr. Mitt. 76, 217–233. https://doi.org/10.5169/seals- 57699.

Butler, R.W.H., Tavarnelli, E., Grasso, M., 2006. Structural inheritance in mountain belts: an Alpine–Apennine perspective. J. Struct. Geol. 28, 1893–1908. https://doi.org/10.1016/j.jsg.2006.09.006.

Butler, J.P., Beaumont, C., Jamieson, R.A., 2013. The Alps 1: a working geodynamic model for burial and exhumation of (ultra)high pressure rocks in Alpine-type orogens. Earth Planet. Sci. Lett. 377, 114–131.

Cadoppi, P., 1988. Osservazioni sui granitoidi nel settore settentrionale del Massiccio Dora-Maira (Val Sangone e Val Susa). Rend. Soc. Geol. It. 11, 175–178 (in Italian).

Cadoppi, P., 1990. Geologia del basamento cristallino nel settore settentrionale del massiccio dora-maira (Alpi Occidentali). Ph.D. thesis, University of Torino, p. 208 (in Italian).

Cadoppi, P., Tallone, S., 1992. Structural and lithostratigraphic heterogeneity of the northern part of Dora-Maira massif (Western Alps). Atti Tic. Sci. Terra 35, 9–18.

Cadoppi, P., Castelletto, M., Sacchi, R., Baggio, P., Carraro, F., Giraud, V., 2002. Note illustrative della Carta Geologica d'Italia alla scala 1:50.000, Foglio 154, Susa. Servizio Geologico. d'Italia (in Italian).

Cadoppi, P., Camanni, G., Balestro, G., Perrone, G., 2016. Geology of the Fontane talc mineralization (Germanasca valley, Italian Western Alps). J. Maps 12 (5), 1170–1177. https://doi.org/10.1080/17445647. 2016.1142480.

Casini, L., Cuccuru, S., Puccini, A., Oggiano, G., Rossi, P., 2015. Evolution of the Corsica-Sardinia batholith and late-orogenic shearing of the Variscides. Tectonophysics 646, 65–78. https://doi.org/10.1016/j.tecto.2015.01.017.

Cassinis, G., Perotti, C., Santi, G., 2018. Post-Variscan Verrucano-like deposits in Italy, and the onset of the alpine tectono-sedimentary cycle. Earth Sci. Rev. 185, 476–497.

Castelli, D., Rolfo, F., Groppo, C., Compagnoni, R., 2007. Impure marbles from the UHP Brossasco-Isasca Unit (Dora-Maira Massif, western Alps): evidence for Alpine equilibration in the diamond stability field and evaluation of the $X(CO_2)$ fluid evolution. J. Metam. Geol. 25 (6), 587–603.

Chen, Y.X., Schertl, H.P., Zheng, Y.F., Huang, F., Zhou, K., Gong, Y.Z., 2016. Mg–O isotopes trace the origin of Mg-rich fluids in the deeply subducted continental crust of Western Alps. Earth Planet. Sci. Lett. 456, 157–167. https://doi.org/10.1016/j.epsl.2016.09.010.

Chen, Y.X., Zhou, K., He, Q., Zheng, Y.F., Schertl, H.P., Chen, K., 2023. First finding of continental deep subduction in the Sesia Zone of the Western Alps and implications for subduction dynamics. Nat. Sci Rev. 10 (5), 2178–2194. https://doi.org/10.1093/nsr/nwad023.

Chopin, C., 1984. Coesite and pure pyrope in high-grade blueschists of the Western Alps: a first record and some consequences. Contrib. Mineral. Petrol. 86, 107–118. https://doi.org/10.1007/BF00381838.

Chopin, C., Henry, C., Michard, A., 1991. Geology and petrology of the coesite bearing terrain, Dora Maira massif, Western Alps. Europ. J. Mineral. 3 (2), 263–291. https://doi.org/10.1127/ejm/3/2/0263.

Cocco, F., Loi, A., Funedda, A., Casini, L., Ghienne, J.F., Pillola, G.L., Vidal, M., Meloni, M.A., Oggiano, G., 2023. Ordovician tectonics of the South European Variscan Realm: new insights from Sardinia. Int. J. Earth Sci. 112 (1), 321–344.

Cohen, K.M., Finney, S.C., Gibbard, P.L., Fan, J.X., 2013. The ICS international chronostratigraphic chart. [updated 2025]. Episodes 36 (3), 199–204.

Compagnoni, R., Borghi, A., Cadoppi, P., Ferrando, S., Gattiglio, M., Ruffini, R., 2003. The abundance of 47 elements and petrovolumetric models of the crust in the Susa Valley, Western Alps. Ac. Naz. Sci. XL 32, 69–96.

Compagnoni, R., Rolfo, F., Groppo, C., Hirajima, T., Turello, R., 2012. Geological map of the ultra-high pressure Brossasco-Isasca unit (Western Alps, Italy). J. Maps 8 (4), 465–472. https://doi.org/10.1080/17445647.2012.744367.

Cortesogno, L., Dallagiovanna, G., Gaggero, L., Seno, S., Vanossi, M., 1998. Tettonica e vulcanismo tardo-Paleozoici nel dominio prepiemontese delle Alpi Liguri: La testimonianza della successione del Colle Scravaion. Atti Tic. Sci. Terra 7, 17–26 (in Italian).

Costamagna, L.G., 2024. The Triassic Buntsandstein sedimentary basins of Sardinia (Italy) and their transition to the Brianzonese Ridge (W Alps): crossroads through the W-Tethys areas. J. Geol. Soc. 182 (2), jgs2024-088. https://doi.org/10.1144/jgs2024-088.

Coward, M.P., Dietrich, D., 1989. Alpine tectonics-an overview. In: Coward, M.P., Dietrich, D., Park, R.G. (Eds.), Alpine Tectonics. Geol. Society 45, 1–29. https://doi.org/10.1144/gsl.sp.1989.045.01.01.

Cruciani, G., Franceschelli, M., Musumeci, G., Spani, M.E., Tiepolo, M., 2013. U-Pb zircon dating and nature of metavolcanics and metarkoses from the Monte Grighini Unit: new insights on late Ordovician magmatism in the Variscan belt in Sardinia, Italy. Int. J. Earth Sci. 102 (8), 2077–2096.

d'Atri, A., Piana, F., Barale, L., Bertok, C., Martire, L., 2016. Geological setting of the southern termination of Western Alps. Int. J. Earth Sci. 105 (6), 1831–1858.

Dalla Giovanna, G., Gaggero, L., Maino, M., Seno, S., Tiepolo, M., 2009. U-Pb zircon ages for post-Variscan volcanism in the Ligurian Alps (Northern Italy). J. Geol. Soc. 166 (1), 101–114. https://doi.org/10.1144/0016-76492008-027.

Dal Piaz, G.V., 1999. The Austroalpine-Piedmont nappe stack and the puzzle of Alpine Tethys. Mem. Sci. Geol. 51 (1), 155–176.

Dal Piaz, G.V., Bistacchi, A., Massironi, M., 2003. Geological outline of the Alps. Episodes 26 (3), 175–180 https://doi.org/10.18814/epiiugs/2003/v26i3/004.

Decarlis, A., Lualdi, L., 2008. Late Triassic-Early Jurassic paleokarst from the Ligurian Alps and its geological significance (Siderolitico Auct., Ligurian Briançonnais domain). Swiss J. Geosci. 101 (3), 579–593. https://doi.org/10.1007/s00015-008-1302-0.

Decarlis, A., Dallagiovanna, G., Lualdi, A., Maino, M., Seno, S., 2013. Stratigraphic evolution in the Ligurian Alps between Variscan heritages and the Alpine Tethys opening: a review. Earth Sci. Rev. 125 (145), 43–68.

De Togni, M., Balestro, G., Rubatto, D., Castelli, D., Gattiglio, M., Festa, A., 2024. Late Jurassic magmatism in the Ligurian-Piedmont Ocean constrained by zircon ages of mafic and felsic meta-intrusives. Terra Nova 36 (5), 403–413. https://doi.org/10.1111/ter.12723.

Diamanti, R., Awais, M., Camanni, G., D'Antonio, M., Della Porta, G., Renzo, V., Graziano, S., Iannace, A., Kylander-Clark, A., Vitale, E., Vitale, S., 2024. Fault-controlled saddle dolomitization during the late Triassic Pangea breakup in the southern Adria domain (Southern Italy). Marine Petrol. Geol. 174, 107216. https://doi.org/10.1016/j.marpetgeo.2024.107216.

Di Vincenzo, G., Tonarini, S., Lombardo, B., Castelli, D., Ottolini, L., 2006. Comparison of ^{40}Ar-^{39}Ar and Rb-Sr data on phengites from the UHP Brossasco-Isasca unit (Dora Maira Massif, Italy): Implications for dating white mica. J. Petrol. 47 (4), 1439–1465. https://doi.org/10.1093/petrology/egl018.

Dumont, T., Lemoine, M., Tricart, P., 1984. Tectonique synsédimentairetriasico–jurassique et rifting téthysien dans l'unité prépiémontaise deRochebrune au Sud–Est de Briançon. Bull. Soc. Géol. France 26 (5), 921–933 (in French with English abstract). https://doi.org/10.2113/gssgfbull.S7-XXVI.5.921.

Elter, G., 1972. Contribution a la connaissance du Briançonnais interne et de la bordure piémontaise dans les Alpes Graies nord-orientales et considérations sur les rapports entre les zones du Briançonnais et des Schistes Lustrés. Mem. Inst. Geol. Mineral. Univ. Padova 28, 1–19 (in French).

Erdős, Z., Huismans, R., Beek, P., Thieulot, C., 2014. Extensional inheritance and surface processes as controlling factors of mountain belt structure. J. Geophysic. Res. Solid Earth. 119 (12), 9042–9061. https://doi.org/10.1002/2014JB011408.

Faure, J.L., Megard-Galli, J., 1988. L'émersion jurassique en Briançonnais: sédimentation continentale et fracturation distensive. Bull. Soc. Géol. France 8 (4), 681–692. in French with English abstract).

Ferrando, S., Bernoulli, D., Compagnoni, R., 2004. The Canavese zone (internal Western Alps): a distal margin of Adria. Schweiz. Mineral. Petrogr. Mitt. 84 (3), 237–256.

Ferrando, S., Groppo, C., Frezzotti, M.L., Castelli, D., Proyer, A., 2017. Dissolving dolomite in a stable UHP mineral assemblage: evidence from Cal-Dol marbles of the Dora- Maira Massif (Italian Western Alps). Am. Mineralogist 102 (1), 42–60.

Festa, A., Balestro, G., Borghi, A., De Caroli, S., Succo, A., 2020. The role of structural inheritance in continental break-up and exhumation of Alpine Tethyan mantle (Canavese Zone, Western Alps). Geosci. Front. 11 (1), 167–188. https://doi.org/10.1016/j.gsf.2018.11.007.

Festa, A., Meneghini, F., Balestro, G., Pandolfi, L., Tartarotti, P., Dilek, Y., Marroni, M., 2021. Comparative analysis of the sedimentary cover units of the Jurassic Western Tethys Ophiolites in the Northern Apennines and Western Alps (Italy): processes of the formation of mass transport and chaotic deposits during sea-floor spreading and subduction zone tectonics. J. Geology 129, 533–561. https://doi.org/10.1086/716498.

Franchi, S., 1898. Sull'età mesozoica della zona delle pietre verdi nelle Alpi Occidentali. Boll. r. Comit. Geol. It. 29, 173–247 (in Italian).

Franke, W., Cocks, L.R.M., Torsvik, T.H., 2019. Detrital zircons and the interpretation of palaeogeography, with the Variscan Orogeny as an example. Geol. Mag. 157 (4), 690–694. https://doi.org/10.1017/S0016756819000943.

Frasca, G., Manatschal, G., Chenin, P., 2024. Kinematic reconstruction of the Alpine Tethys and surrounding Mesozoic rifted margins. Int. J. Earth Sci. 113, 1053–1065. https://doi.org/10.1007/s00531-024-02407-9.

Fudral, S., Deville, E., Pognante, U., Gay, M., Fregolent, G., Lorenzini, S., Robert, D., Nicoud, G., Black, C., Jayko, A., Jaillard, E., Bertrand, J.M., Forno, M.G., Massazza, G., 1994. Lanslebourg-Mont-d'Ambin— Carte géologique de la France a' 1/50 000. Ministére de l'industrie, B.R.G.M (in French).

Fudral, S., 1996. Etude géologique de la suture téthysienne dans les Alpes franco-italiennes nord-occidentales de la Doire Ripaire (Italie) à la région de Bourg-Saint-Maurice (France). Ph.D. thesis, Tectonique, Université de Savoie, p. 306 (in French).

Gambino, F., Borghi, A., d'Atri, A., Martire, L., Cavallo, M., Appolonia, L., Croveri, P., 2019. Minero-petrographic characterization of Chianocco marble employed for Palazzo Madama Façade in Turin (Northwest Italy). Sustainability 11 (15), 4229. https://doi.org/10.3390/su11154229.

Gasco, I., Gattiglio, M., Borghi, A., 2011. Lithostratigraphic setting and P–T metamorphic evolution for the Dora Maira Massif along the Piedmont Zone boundary (middle Susa Valley, NW Alps). Int. J. Earth Sci. 100 (5), 1065–1085. https://doi.org/10.1007/s00531-011-0640-8.

Gasco, I., Gattiglio, M., Borghi, A., 2013. Review of metamorphic and kinematic data from internal crystalline massifs (Western Alps): PTt paths and exhumation history. J. Geodyn. 63, 1–19. https://doi.org/10.1016/j.jog.2012.09.006.

Gasser, D., Grenne, T., Corfu, F., Bøe, R., Røhr, T., Slagstad, T., 2022. Concurrent MORB-type and ultrapotassic volcanism in an extensional basin along the Laurentian Iapetus margin: Tectonomagmatic response to Ordovician arc-continent collision and subduction polarity flip. Geol. Soc. Am. Bull. 134 (7–8), 1635–1659. https://doi.org/10.1130/B36113.1.

Gauthiez- Putallaz, L., Rubatto, D., Hermann, J., 2016. Dating prograde fluid pulses during subduction by in situ U–Pb and oxygen isotope analysis. Contrib. Mineral. Petrol. 171 (2), 15.

Gebauer, D., Schertl, H.P., Brix, M., Schreyer, W., 1997. 35 Ma old ultrahigh-pressure metamorphism and evidence for very rapid exhumation in the Dora Maira Massif, Western Alps. Lithos 41 (1–3), 5–24.

Ghignone, S., Gattiglio, M., Balestro, G., Borghi, A., 2020. Geology of the Susa Shear Zone (Susa Valley, Western Alps). J. Maps 16 (2), 79–86.

Gilotti, J.A., McClelland, W.C., Schorn, S., Compagnoni, R., Coble, M.A., 2023. Provenance, protolith and metamorphic ages of jadeite-bearing orthogneiss and host paragneiss at Tavagnasco, the Sesia Zone, lower Aosta Valley, Italy. Europ. J. Mineral. 35 (4), 645–658.

Godard, G., 2009. Two orogenic cycles in eclogite-facies gneisses of the Southern Armorican Massif (France). Europ. J. Mineral. 21 (6), 1173–1190.

Groppo, C., Rolfo, F., Castelli, D., 2007. Pre-Alpine HT mineral relics in impure marbles from the UHP Brossasco-Isasca Unit (Dora-Maira Massif, western Alps). Periodico Di Mineralogia 76 (3), 155–168.

Groppo, C., Ferrando, S., Gilio, M., Botta, S., Nosenzo, F., Balestro, G., Festa, A., Rolfo, F., 2019. What's in the sandwich? New P-T constraints for the (U) HP nappe stack of southern Dora-Maira Massif (Western Alps). Europ. J. Mineral. 31, 665–683. https://doi.org/10.1127/ejm/2019/0031-2860.

Groppo, C., Rapa, G., Frezzotti, M.L., Rolfo, F., 2021. The fate of calcareous pelites in collisional orogens. J. Metamorph. Geol. 39 (2), 181–207. https://doi.org/10.1111/jmg.12568.

Groppo, C., Ferrando, S., Tursi, F., Rolfo, F., 2025. A new UHPHP tectono-metamorphic architecture for the southern Dora-Maira Massif nappe stack (western Alps) based on petrologic and microstructural evidence. J. Metamorph. Geol. 43 (4), 359–383. https://doi.org/10.1111/jmg.12812.

Handy, M., Schmid, S., Bousquet, R., Kissling, E., Bernoulli, D., 2010. Reconciling plate- tectonic reconstructuons of Alpine Tethys with the geological-geophysical record of spreading and subduction in the Alps. Earth Sci. Rev. 102 (3-4), 121–158. https://doi.org/10. 1016/j.earscirev.2010.06.002.

Henry, C., Michard, A., Chopin, C., 1993. Geometry and structural evolution of ultra-high pressure and high pressure rocks from the Dora-Maira massif, Western Alps, Italy. J. Struct. Geol. 15 (8), 965–981. https://doi.org/10.1016/0191-8141(93)90170-F.

Hermann, J., 2003. Experimental evidence for diamond- facies metamorphism in the Dora-Maira massif. Lithos 70 (3–4), 163–182.

Keller, L., Schmid, S., 2001. On the kinematics of shearing near the top of the Monte Rosa nappe and the nature of the Furgg zone in Val Loranco (Antrona valley, N. Italy): Tectonometamorphic and paleogeographical consequences. Schweiz. Mineral. Petrogr. Mitt. 81, 347–367.

Lemoine, M., Bas, T., Arnaud-Vanneau, A., Arnaud, H., Dumont, T., Gidon, M., Bourbon, M., de Graciansky, P.-C., Rudkiewicz, J.-L., Mégard-Galli, J., Tricart, P., 1986. The continental margin of the Mesozoic Tethys in the Western Alps. Marine Geol. 3 (3), 179–199.

Lemoine, M., Trümpy, R., 1987. Pre-oceanic rifting in the Alps. Tectonophysics 133 (3–4), 305–320.

Linnemann, U., Gerdes, A., Drost, K., Buschmann, B., 2007. The continuum between Cadomian orogenesis and opening of the Rheic Ocean: Constraints from LA-ICPMS U-Pb zircon dating and analysis of plate-tectonic setting (Saxo-Thuringian zone, north-eastern Bohemian Massif, Germany). In: Linnemann, U., Nance, R.D., Kraft, P., Zulauf, G. (Eds), The Evolution of the Rheic Ocean: from Avalonian Cadomian Active Margin to Alleghenian-Variscan Collision. Geol. Soc. Am. Sp. 423, 61–96.

Linnemann, U., 2025. Inside Pangea: A brief introduction to the Variscan Orogen in central Europe. In: Linnemann, U. (Ed), The Variscan Orogen of Central Europe. Springer, 1–11. https://doi.org/10.1007/978-3-031-82911-6.

Lualdi, A., Bianchi, U., 1990. La Formazione di Costa Losera: una nuova unità stratigrafica dell'Anisico delle Alpi Liguri (Brianzonese e Prepiemontese). Att. Tic. Sci. Terra 33, 33–62 (in Italian).

Ludwig, K.R., 2003. Isoplot/EX, version 3, A geo-chronological toolkit for Microsoft Excel: Berkeley Geochronology Center Special Publication, 4.

Luisier, C., Baumgartner, L., Putlitz, B., Vennemann, T., 2021. Whiteschist genesis through metasomatism and metamorphism in the Monte Rosa nappe (Western Alps). Contrib. Mineral. Petrol. 176, 10. https://doi.org/10.1007/s00410-020-01759-0.

Maino, M., Gaggero, L., Langone, A., Seno, S., Fanning, M., 2018. Cambro-Silurian magmatisms at the northern Gondwana margin (Penninic basement of the Ligurian Alps). Geosci. Front. 10 (1), 315–330.

Malusà, G.M., Faccenna, C., Garzanti, E., Polino, R., 2011. Divergence in subduction zones and exhumation of high pressure rocks (Eocene Western Alps). Earth Planet. Sci. Lett. 310 (1–2), 21–32. https://doi.org/10.1016/j.epsl.2011.08.002.

Manatschal, G., Chenin, P., Haupert, I., Masini, E., Frasca, G., Decarlis, A., 2022. The importance of rift inheritance in understanding the early collisional evolution of the Western Alps. Geosciences 12 (12), 1–43. https://doi.org/10.3390/geosciences12120434.

Manzotti, P., Pitra, P., Langlade, J., Ballèvre, M., 2015. Constraining P-T conditions during thrusting of a higher pressure unit over a lower pressure one (Gran Paradiso, Western Alps). J. Metamorph. Geol. 33 (9), 981–1022.

Manzotti, P., Ballèvre, M., Poujol, M., 2016. Detrital zircon geochronology in the Dora-Maira and zone Houillère: a record of sediment travel paths in the Carboniferous. Terra Nova 28 (4), 279–288. https://doi.org/10.1111/ter.12219.

Manzotti, P., Schiavi, F., Nosenzo, F., Pitra, P., Ballèvre, M., 2022. A journey towards the forbidden zone: a new cold UHP unit in the Dora-Maira Massif (Western Alps). Contrib. Mineral. Petrol. 177 (6), 1–22. https://doi.org/10.1007/s00410-022-01923-8.

Manzotti, P., Millonig, L.J., Gerdes, A., Whitehouse, M.J., Jeon, H., Poujol, M., Ballèvre, M., 2025a. Protolith age, and timing of burial and exhumation of the UHP Chasteiran Unit (Dora-Maira Massif, Western Alps), constrained by zircon, garnet and rutile petrochronology. Lithos 496–497, 107951. https://doi.org/10.1016/j.lithos.2025.107951.

Manzotti, P., Schiavi, F., Ballèvre, M., Nosenzo, F., 2025b. Garnet growth across the quartz–coesite transition in metapelites: equilibrium vs. kinetics. Europ. J. Mineral. 37 (4), 455–482. https://doi.org/10.5194/ejm-37-455-2025.

Marroni, M., Pandolfi, L., 2007. The architecture of the Jurassic Ligure-Piemontese oceanic basin: tentative reconstruction along the Northern Apennine–Alpine Corsica transect. Int. J. Earth Sci. 96 (6), 1059–1078. https://doi.org/10.1007/s00531-006-0163-x.

Marroni, M., Meneghini, F., Pandolfi, L., 2010. Anatomy of the Ligure-Piemontese subduction system: evidence from late Cretaceous-middle Eocene convergent margin deposits in the Northern Apennines, Italy. Int. Geol. Rev. 52, 1160–1192. https://doi.org/10.1080/00206810903545493.

Marroni, M., Meneghini, F., Pandolfi, L., 2017. A revised subduction inception model to explain the late Cretaceous, double-vergent orogen in the precollisional Western Tethys: evidence from the Northern Apennines. Tectonics 36 (10), 2227–2249. https://doi.org/10.1002/2017TC004627.

Marthaler, M., Fudral, S., Deville, E., Rampnoux, J.P., 1986. Mise en évidence du Crétacé supérieur dans la couverture septentrionale de Dora-Maira, région de

Suse, Italie (Alpes Occidentales). Conséquences paléogéographyques et structurales. CR Acad. Sci. Paris 302 (2), 91–96 (in French).
Masini, E., Manatschal, G., Mohn, G., 2013. The Alpine Tethys rifted margins: Reconciling old and new ideas to understand the stratigraphic architecture of magma-poor rifted margins. Sedimenology 60 (1), 174–196. https://doi.org/10.1111/sed.12017.
Michard, A., Vialon, P., 1966. Permo-Trias, Permien s.1. Et Permo-Carbonifère metamorphises des Alpes Cottiennes internes: Les facies "Verrucano" et les series volcano-detritiques du Massif Dora-Maira. Atti del Symposium sul Verrucano (Pisa, Settembre 1965). Soc. Toscana Sci. Nat. 116–135 (in French).
Michard, A., 1967. Etudes géologiques dans les zones internes des Alpes cottiennes. Ph.D. thesis, Université de Paris, p. 447 (in French).
Michard, A., Chopin, C., Henry, C., 1993. Compression versus extension in the exhumation of the Dora-Maira coesite-bearing unit, Western Alps, Italy. Tectonophysics 221, 173–193. https://doi.org/10.1016/0040-1951(93)90331-D.
Michard, A., Avigad, D., Goffé, B., Chopin, C., 2004. The high-pressure metamorphic front of the south Western Alps (Ubaye-Maira transect, France, Italy). Schweiz. Min. Petr. Mitt. 84 (3), 215–235.
Michard, A., Schmid, S.M., Lahfid, A., Ballèvre, M., Manzotti, P., Chopin, C., Iaccarino, S., Dana, D., 2022. The Maira-Sampeyre and Val Grana allochthons (south Western Alps): review and new data on the tectonometamorphic evolution of the Briançonnais distal Margin. Swiss J. Geosci. 115 (1), 19.
Mohn, G., Manatschal, G., Beltrando, M., Masini, E., Kusznir, N., 2012. Necking of continental crust in magma-poor rifted margins: evidence from the fossil Alpine Tethys margins. Tectonics 31 (1), TC1012. https://doi.org/10.1029/2011TC002961.
Mohn, G., Manatschal, G., Beltrando, M., Haupert, I., 2014. The role of rift-inherited hyper-extension in Alpine-type orogens. Terra Nova 26 (5), 347–353. https://doi.org/10.1111/ter.12104.
Nesbitt, H.W., Young, G.M., 1982. Early Proterozoic climates and plate motions inferred from major element chemistry of lutites. Nature 299 (5885), 715–717.
Nosenzo, F., Manzotti, P., Poujol, M., Ballèvre, M., Langlade, J., 2022. A window into an older orogenic cycle: P-T conditions and timing of the pre-Alpine history of the Dora-Maira Massif (Western Alps). J. Metamorph. Geol. 40 (4), 789–821.
Nosenzo, F., Manzotti, P., Krona, M., Ballèvre, M., Poujol, M., 2024. Tectonic architecture of the northern Dora- Maira Massif (Western Alps, Italy): field and geochronological data. Swiss J. Geosci. 117 (1), 1–33. https://doi.org/10.1186/s00015-024-00459-2.
Pantet, A., Epard, J.L., Masson, H., 2020. Mimicking Alpine thrusts by passive deformation of synsedimentary normal faults: a record of the Jurassic extension of the European margin (Mont Fort nappe, Pennine Alps). Swiss J. Geosci. 113 (1), 13.
Perrone, G., Eva, E., Solarino, S., Cadoppi, P., Balestro, G., Fioraso, G., Tallone, S., 2010. Seismotectonic investigations in the inner Cottian Alps (Italian Western Alps): an integrated approach. Tectonophysics 496 (1–4), 1–16. https://doi.org/10.1016/j.tecto.2010.09.009.
Petti, F.M., Furrer, H., Collo, E., Martinetto, E., Bernardi, M., Delfino, M., Romano, M., Piazza, M., 2020. Archosauriform footprints in the Lower Triassic of Western Alps and their role in understanding the effects of the Permian-Triassic hyperthermal. Peer J. 8 (1), 10522.
Pfiffner, O.A., 2017. Thick-skinned and thin-skinned tectonics: a global perspective. Geosciences 7 (3), 71.
Platt, J.P., 1986. Dynamics of orogenic wedges and the uplift of high-pressure metamorphic rocks. Geol. Soc. Am. Bull. 97 (9), 1037–1053. https://doi.org/10.1098/rsta.1987.0006.
Platt, J.P., Behrmann, J., Cunningham, P.C., Dewey, J., Helman, M., Parish, M., Shepley, M., Wallis, S., Western, P., 1989. Kinematics of the Alpine Arc and the motion history of Adria. Nature 337, 158–161. https://doi.org/10.1038/337158a0.
Pognante, U., 1980. Preliminary data on the Piemonte ophiolite nappe in the lower Val Susa-Val Chisone area, Italian Western Alps. Ofioliti 5 (2–3), 221–240.
Pognante, U., Sandrone, R., 1989. Eclogites in the Northern Dora-Maira Nappe (Western Alps, Italy). Mineral. Petrol. 40 (1), 57–71.
Polino, R., Dal Piaz, G.V., Gosso, G., 1990. Tectonic erosion at the Adria margin and accretionary processes for the Cretaceous orogeny of the Alps. Soc. Geol. It. 156, 345–367.
Ribes, C., Manatschal, G., Ghienne, J.F., Karner, G.D., Johnson, C.A., Figueredo, P.H., Incerpi, N., Epin, M.E., 2019. The syn-rift stratigraphic record across a fossil hyper-extended rifted margin: the example of the northwestern Adriatic margin exposed in the Central Alps. Int. J. Earth Sci. 108, 2071–2095. https://doi.org/10.1007/s00531-019-01750-6.
Rosenbaum, G., Lister, G.S., 2005. The Western Alps from the Jurassic to Oligocene: spatio-temporal constraints and evolutionary reconstructions. Earth Sci. Rev. 69 (3–4), 281–306. https://doi.org/10.1016/j.earscirev. 2004.10.001.
Rosenberg, C., Bellahsen, N., 2024. Geodynamics of the Alps 2: Pre-collisional Processes. Wiley,, pp. 1–365. https://doi.org/10.1002/9781394299539.
Rubatto, D., Hermann, J., 2001. Exhumation as fast as subduction? Geology 29 (1), 3–6.
Rubatto, D., Ferrando, S., Compagnoni, R., Lombardo, B., 2010. Carboniferous high-pressure metamorphism of Ordovician protoliths in the Argentera Massif (Italy), Southern European Variscan Belt. Lithos 116 (1–2), 65–76. https://doi.org/10.1016/j.lithos.2009.12.013.
Rubatto, D., 2017. Zircon: the metamorphic mineral. Rev. Mineral. Geochem. 83 (1), 261–296. https://doi.org/10.2138/rmg.2017.83.9.
Santi, G., Lualdi, A., Decarlis, A., Nicosia, U., Ronchi, A., 2015. Chirotheriid footprints from the Lower-Middle Triassic of the Briançonnais Domain (Pelite di Case Valmarenca, Western Liguria, NW Italy). Boll. Soc. Paleont. It. 54 (2), 82.
Sandrone, R., Cadoppi, P., Sacchi, R., Vialon, P., 1993. The Dora-Maira massif. In: Von Raumer, J.F., Neubauer, F. (Eds.), Pre-Mesozoic Geology in the Alps. Springer, pp. 317–325.
Schettino, A., Turco, E., 2011. Tectonic history of the western Tethys since the late Triassic. Geol. Soc. Am. Bull. 123 (1–2), 89–105. https://doi.org/10.1130/B30064.1.
Schmid, S.M., Fugenschu, H.B., Klissing, E., Schuster, R., 2004. Tectonic map and overall architecture of the Alpine orogen. Ecl. Geol. Helv. 97 (1), 93–117. https://doi.org/10.1007/s00015-004-1113-x.
Schmid, S.M., Kissling, E., Diehl, T., Van Hinsbergen, D.J.J., Molli, G., 2017. Ivrea mantle wedge, arc of the Western Alps, and kinematic evolution of the Alps-Apennines orogenic system. Swiss J. Geosci. 110 (2), 581–612. https://doi.org/10.1007/s00015-016-0237-0.
Siegesmund, S., Oriolo, S., Schulz, B., Heinrichs, T., Basei, M.A.S., Lammerer, B., 2021. The birth of the Alps: Ediacaran to Paleozoic accretionary processes and crustal growth along the northern Gondwana margin. Int. J. Earth Sci. 110 (4), 1321–1348. https://doi.org/10.1007/s00531-021-02019-7.
Syahputra, R., Žák, J., Tomek, F., Kachlík, V., 2023. Hot plutonism in a cold accretionary wedge: what terminated the Cadomian orogeny at the northern periphery of Gondwana? Precambrian Res. 390, 107041. https://doi.org/10.1016/j.precamres.2023.107041.
Spalla, M.I., Zanoni, D., Marotta, A.M., Rebay, G., Roda, M., Zucali, M., Gosso, G., 2014. The transition from Variscan collision to continental break-up in the Alps: Insights from the comparison between natural data and numerical model predictions. Geol. Soc. Sp. Publ. 405, 363–400.
Stampfli, G.M., von Raumer, J.F., Borel, G.D., 2002. The Palaeozoic evolution of pre-Variscan terranes: from Gondwana to the Variscan collision. In: Martinez-Catalan, J.R., Hatcher, R.D., Arenas, R., Diaz Garcia, F. (Eds.), Variscan-Appalachian Dynamics: The Building of the Late Palaeozoic Basement. Geol. Soc. Am. Spec. Paper 364, 263–280.
Tallone, S., 1988. Osservazioni litostratigrafiche e strutturali nella copertura del Massiccio Dora-Maira lungo il fianco sinistro della Valle di Susa. Rend. Soc. Geol. It. 11, 171–174 (in Italian).
Tallone, S., 1990. Il Dora-Maira settentrionale e le sue coperture mesozoiche: relazioni tra litostratigrafia, struttura ed evoluzione metamorfica. Ph.D. thesis, University of Torino, p. 147 (in Italian).
Tamang, S., Groppo, C., Girault, F., Perrier, F., Rolfo, F., 2024. Metamorphism of dolomitic and magnesitic rocks in collisional orogens and implications for orogenic CO_2 degassing. J. Petrology 65 (4), 271–297.
Tavani, S., Granado, P., Corradetti, A., Camanni, G., Vignaroli, G., Manatschal, G., Mazzoli, S., Munoz, J.A., Parente, M., 2021. Rift inheritance controls the switch from thin- to thick-skinned thrusting and basal décollement re-localization at the subduction-to-collision transition. Geol. Soc. Am. Bull. 133 (9–10), 2157–2170. https://doi.org/10.1130/B35800.1.
Thiéblemont, D., Jacob, J., Lach, P., Guerrot, C., Leguérinel, M., 2023. First report of an Ediacarian basement in the Western Alps: the Serre Chevalier crystalline unit (Briançonnais domain, France). BSGF - Earth Sci. Bull. 194 (1), 16. https://doi.org/10.1051/bsgf/2023011.
Tilton, G.R., Schreyer, W., Schertl, H.P., 1989. Pb–Sr–Nd isotopic behaviour of deeply subducted crustal rocks from the Dora Maira massif, Western Alps Italy. Geoch. Cosmochimica Acta 53 (6), 1391–1400.
Tricart, P., Bourbon, M., Chenet, P., Cros, P., Delorme, M., Dumont, T., Graciansky, P., Lemoine, M., Megard-Galli, J., Richez, M., 1988. Tectonique synsedimentaire triassico-jurassique et rifting tethysien dans la nappe brianconnaise de Peyre-Haute (Alpes occidentales). Bull. Soc. Géol. France IV 4, 669–680. https://doi.org/10.2113/gssgfbull.IV.4.669 (in French with English abstract)..
Vanossi, M., 1969. La serie Brianzonese del Salto del Lupo (Liguria Occidentale): osservazione sedimentologico-stratigrafiche. Atti Ist. Geol. Univ. Pavia 20, 3–16 (in Italian).
Vanossi, M., 1974. Analisi stratigrafica-strutturale della zona tra le alte valli del Casotto e dell'Ellero (Alpi Marittime). Atti Ist. Geol. Univ. Pavia 14, 38–72 (in Italian).
Vermeesch, P., 2018. IsoplotR: a free and open toolbox for geochronology. Geosci. Front. 9 (5), 1479–1493.
Vermeesch, P., 2021. Corrigendum to "IsoplotR: a free and open toolbox for geochronology". Geosci. Front. 12 (5), 101227. https://doi.org/10.1016/j.gsf.2021.101227.
Vialon, P., 1966. Étude géologique du massif cristallin Dora-Maira, Alpes cottiennes internes, Italie. Travaux Du Laboratoire De Géologie De Grenoble, Mèmoires 4, 1–282 (in French).
Von Raumer, J.F., Bussy, F., Schaltegger, U., Schulz, B., Stampfli, G.M., 2013. Pre-Mesozoic Alpine basements: their place in the European Paleozoic framework. Geol. Soc. Am. Bull. 125 (1–2), 89–108.
Yang, G., 2022. Subduction initiation triggered by collision: a review based on examples and models. Earth Sci. Rev. 232, 104–129.
Žák, J., Svojtka, M., Nance, R., Murphy, J., 2025. Detrital zircon record of shutdown and migration of Cadomian volcanic arcs in the Bohemian Massif, with implications for Ediacaran to early Cambrian plate kinematics. Precambrian Res. 422, 107786. https://doi.org/10.1016/j.precamres.2025.107786.
Zhou, K., Chen, Y.X., Xiong, J.W., Schertl, H.P., Xia, Z.P., 2023. Fluid effect on zircon O and U-Pb isotopes during ultrahigh-pressure metamorphism: Insights from the Dora-Maira Massif of the Western Alps. Geosci. Front. 14 (5), 101651. https://doi.org/10.1016/j.gsf.2023.101651.